Impact of the sea state on the atmosphere and ocean

Peter A.E.M. Janssen, Oyvind Saetra, Cecilie Wettre, Hans Hersbach, and Jean Bidlot

Abstract

Ocean waves represent the interface between the ocean and the atmosphere, and, therefore, wave models are needed to compute not only the wave spectrum, but also the processes at the air-sea interface that govern the fluxes across the interface.

This was one of the reasons for developing a wave prediction model, called the WAM model, that determines the sea state dependence of the air-sea fluxes. As a first step, the study of the two-way interaction between ocean waves and atmospheric circulation was undertaken. Modest improvements in forecasting waves and winds were obtained, and, as a consequence, since the 29th of June 1998 ECMWF produces weather and ocean wave analyses and forecasts using a coupled IFS-WAM forecasting system.

In this paper, we briefly discuss our recent experience with two-way interaction. Nowadays, there is a substantial impact on weather and wave forecasting, and reasons for this increase in impact are given. A future task is to couple the ocean waves and the ocean circulation. It is argued that prediction of the ocean circulation would benefit from the inclusion of currents in the calculation of fluxes. In addition, it is shown that the thickness of the ocean mixed layer is to a large extent determined by the energy flux associated with breaking ocean waves, and furthermore, the momentum flux is controlled to a lesser extent by breaking waves. Finally, in the presence of ocean waves, many authors have shown that there is an additional force on the mean flow, given by the cross product of the Stokes drift and the Coriolis parameter (Coriolis-Stokes forcing). This would have a large impact on the Ekman transport. It is pointed out, however, that in a Eulerian frame there is also a surface drift caused by the waves which exactly cancels the total momentum of the Coriolis-Stokes forcing. There may still be an impact of the Stokes drift on the circulation in the deeper layers of the ocean, but this depends on the interaction of the surface drift and oceanic turbulence.

1 INTRODUCTION.

Ocean waves represent the interface between the ocean and the atmosphere, the two most important systems governing the dynamics of climate and global change. A realistic description of the physical processes occurring at the ocean-atmosphere interface is essential for a reliable determination of the air-sea fluxes of momentum, sensible and latent heat, CO_2 and other trace gases, and aerosols. It is known that the wave field is intimately involved in these exchange processes, and, therefore, wave models are needed to compute not only the wave spectrum, but also the processes at the air-sea interface that govern the fluxes across the interface.

In the context of this extensive programme, a wave prediction system, called the WAM model, was developed that determines the sea state dependence of the air-sea fluxes (Komen et al, 1994). As a first step, the study of the two-way interaction between ocean waves and atmospheric circulation was undertaken. This interaction takes place on a relatively short time scale of a few days. Modest improvements in medium-range forecasting of waves and winds were obtained and, as a consequence, since the 29th of June 1998 ECMWF has been producing weather and ocean wave analyses and forecasts, using a coupled IFS-WAM forecasting system. On a seasonal time scale, depending on spatial resolution, however, a more substantial impact of ocean waves on the atmospheric climate was found (Janssen and Viterbo, 1996).

In this paper, we briefly discuss our recent experience with two-way interaction. Nowadays, this interaction has a substantial impact on weather and wave forecasting, one of the reasons being considerable increases in the spatial resolution of the atmospheric model which allows a more realistic representation of the small scales. These are the spatial scales that matter for small-scale air-sea interaction.

The next step in the development of one model for our geosphere is to study the impact of the sea state on the ocean circulation. These studies are only beginning and therefore we are in this respect still in an exploration phase. Nevertheless, already some promising developments may be reported.

There are a number of ways in which the sea state could affect the evolution of the ocean state. In the usual description of the ocean the momentum of the ocean waves is not taken into account, nevertheless a considerable list of authors (Hasselmann, 1970; Weber, 1983; Jenkins, 1987a; Xu and Bowen, 1994; McWilliams and Restrepo, 1999) have pointed out that in a rotating ocean the ocean waves excert a wave-induced stress on the Eulerian mean flow which results in a force equal to $\vec{u}_s \times \vec{f}$, where $\vec{f}$ is the Coriolis parameter, and $\vec{u}_s$ equals the Stokes drift. This additional force has a considerable impact on the Ekman turning of the surface current (Weber, 1983; Jenkins, 1987b; Polton et al, 2003). However, it is not clear whether the introduction of this additional force is appropriate, for the simple observation that conservation of momentum seems to be

All authors are with E.C.M.W.F., Shinfield Park, Reading, RG2 9AX, U.K.

violated. In this paper we discuss how to restore conservation of momentum by pointing out that in a Eulerian frame there is a surface drift which exactly cancels the momentum corresponding to the $\vec{u}_s \times \vec{f}$ term. Hence, inclusion of the surface drift will leave the Ekman transport unaffected, but the Ekman turning at the surface is affected by the presence of ocean waves. Depending on how one models the interaction between surface drift and turbulence one may even find considerable effects of the Stokes drift in the deeper layers of the ocean. Polton et al (2003) have shown an impressive agreement with observed currents at the Ekman depth.

In addition, we study the role ocean waves have in the transfer of momentum and energy to the ocean. In the first place, the roughness at the sea surface and hence the atmosheric flux provided by the atmosphere to the ocean waves is sea-state dependent. This sea-state dependence of the surface stress has a systematic impact on the temperature distribution of the ocean (Burgers et al, 1995). Regarding momentum and energy transfer to the ocean it is noted that in growing circumstances the ocean waves retain a small part of the momentum and energy (which is spent on wave growth). When ocean waves become swell the excess momentum and energy is lost because dissipation by wave breaking dominates the wind input. Furthermore, the momentum transfer is dominated by the high-frequency part of the spectrum (which are in equilibrium with the wind), hence there are only small differences between the atmospheric stress and the momentum flux to the ocean.

The energy flux is commonly parametrized as being proportional to u_*^3 (with u_* the air-friction velocity) where the proportionality constant is of the order of 5. We show that this is indeed a good approxiation in the generation phase of ocean waves. However, when ocean waves propagate out of the storm area, energy fluxes caused by breaking waves are much larger than as found from the above empirical rule. This is also evident from the monthly mean plots of energy flux and momentum flux of January 2003. The mean energy flux shows a considerable spatial variation of about a factor of 5, generally being small in the Tropics while being larger than the global mean value in the extra-Tropics. In contrast, spatial variations in the monthly mean of the momentum flux are at best 5%.

In the surface layer of the ocean, the energy flux caused by breaking waves gives rise to considerable deviations from the balance between production and dissipation of kinetic energy. Following Mellor and Yamada (1982) and Craig and Banner (1994) this imbalance is compensated by the divergence of the turbulent kinetic energy flux. We have studied some of the properties of the so-called "Mellor-Yamada Level 2 $1/2$" closure. In particular, ignoring effects of stratification and the earth's rotation, we obtain for general mixing length an exact solution for turbulent kinetic energy and current profile.

Finally, following the work of Pacanowski (1987) it is argued that prediction of the ocean circulation would benefit from the inclusion of currents in the calculation of fluxes. We shown this by studying its impact on the climate of the coupled ocean-atmosphere system.

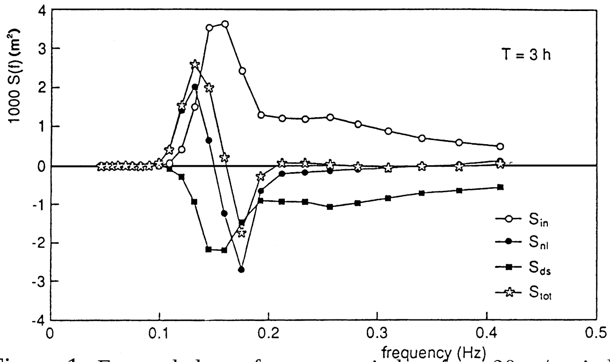

Figure 1: Energy balance for young windsea for a 20 m/s wind speed.

2 IMPACT ON THE ATMOSPHERE.

In this section a brief description of the impact of sea-state dependent drag on the atmospheric circulation is given. The basic idea is described in Janssen (1982) and Janssen (1989) while a parametrization of the sea-state dependent roughness is developed in Janssen (1991). This parametrization is included in WAMCy4 (Komen et al, 1994). A review of the impact on atmospheric circulation is given in Janssen et al (2002).

The basic idea is that momentum transfer from air to sea depends on the sea state because steep waves extract more momentum from the air flow than gentle, smooth waves. Steep waves typically occur in the early stages of wind-wave generation and when a frontal system passes, hence momentum transfer depends on the sea state. In order to account for this effect one needs to calculate the wave-induced stress τ_w which depends on the two-dimensional wave spectrum. Therefore the determination of the wave stress requires the solution of the energy balance equation

$$\frac{\partial}{\partial t}F + \vec{v}_g . \frac{\partial}{\partial \vec{x}}F = S_{in} + S_{nl} + S_{diss} + S_{bot}, \qquad (1)$$

where $F = F(\omega, \theta)$ is the two-dimensional wave spectrum which gives the energy distribution of the ocean waves over angular frequency ω and propagation direction θ. Furthermore, $\vec{v}_g$ is the group velocity and on the right hand side there are four source terms. The first one, S_{in} describes the generation of ocean waves by wind and therefore represents the momentum and energy transfer from air to ocean waves. The third and fourth term describe the dissipation of waves by processes such as white-capping and bottom friction, while the second terms denotes nonlinear transfer by resonant four-wave interactions. The nonlinear transfer conserves total energy and momentum and is important in shaping the wave spectrum and in the down-shift towards lower frequencies. In order to appreciate the role of the respective source terms, in Fig. 1 we have plotted for deep water the directionally averaged source functions S_{in}, S_{nl}, and S_{diss} (as developed for WAMCy4) as function of frequency for young windsea when a 20 m/s wind is blowing for just 3 hours. This figure shows a typical picture of the energy balance for growing ocean waves, namely the intermediate frequencies receive energy from the airflow which is transported by the nonlinear interactions towards the low and high frequencies where it is dissipated by processes such as white capping. The consequence is that the wave spectrum shows a shift of the peak of the spectrum towards lower frequencies, while a considerable enhancement of the peak energy of the spectrum is also noticed in the early stages of wave growth.

At the same time Fig. 1 illustrates the role ocean surface waves play in the interaction of the atmosphere and the ocean, because on the one hand ocean waves receive momentum and energy from the atmosphere through wind input (controlling to some extent the drag of air flow over the oceans), while on the other hand, through wave breaking, the ocean waves transfer energy and momentum to the ocean thereby feeding the turbulent and large-scale motions of the oceans. The energy-conserving nonlinear transfer plays no direct role in this interaction process, although it determines to a large extent the shape of the wave spectrum, and therefore controls energy and momentum fluxes in an indirect way. In equilibrium conditions, the fluxes received by the ocean waves from the atmosphere through the wind input term would balance the fluxes from ocean waves to ocean via wave breaking. However, ocean waves are in general not in an equilibrium state determined by the balance of the three source functions, because advection and unsteadiness are important as well. As a rule of thumb, of the amount of energy gained by wind, about 95% is lost locally to the ocean by wave breaking, while the remaining 5% is either advected away or is spent in local growth. As illustrated in Fig.1, which also shows a plot of the total source function, for young windseas there may, however, be a considerable imbalance, in particular for the low-frequency waves. On the other hand, when wind waves leave a storm area the magnitude of the wind input source function decreases dramatically, while the waves are still sufficiently steep so that white capping is still important. Since dissipation dominates, wave energy will decay and as a consequence momentum and energy flux to the ocean may be larger than the amounts received by the waves from the atmosphere.

It would be of considerable interest to develop a coupled atmosphere- ocean circulation system where the ocean waves are the agent that transfers energy and momentum across the air-sea interface in accordance with the energy balance equation. In this section we shall concentrate on just one aspect of the overall problem, namely the mutual interaction between wind and waves. In the next section we discuss the possible impacts on the ocean circulation.

In the wind-wave interaction problem we only need to know the wave-induced stress τ_w which follows from an integration of the input source function of the energy balance equation (1)

$$\tau_w = \rho_w g \int d\omega d\theta \; S_{in}/c, \tag{2}$$

where c is the phase speed of the gravity waves and ρ_w the water density. Here, it should be realized that wave momentum P and energy density F of the waves are related by $P = F/c$ and the wave stress is the rate of change of total wave momentum by wind input. Because waves grow exponentially fast the source function S_{in} is proportional to the wave spectrum itself. The wave-induced stress is mainly determined by the high-frequency part of the wave spectrum because these are the waves that have the largest growth rate due to wind. Since it is known that the high-frequency spectrum depends on the stage of development of the windsea (for example, young wind waves are steeper than old wind waves) it follows that the wave-induced stress depends on the sea state. Therefore, young wind waves represent a rougher surface than gentle old windsea. The roughness z_0 therefore depends on the sea state and following the work of Janssen (1991) one finds for the roughness length a Charnock relation,

$$z_0 = \alpha u_*^2/g, \tag{3}$$

where the Charnock parameter α depends on the sea state according to

$$\alpha = \frac{\beta}{\sqrt{1 - \tau_w/\tau}}, \; \beta = 0.01, \tag{4}$$

with $\tau = \rho_a u_*^2$ is the surface stress and u_* the friction velocity.

At ECMWF we have developed a coupled ocean-wave, atmosphere model in such a way that the wave model is called as a subroutine from the IFS system. This system was introduced in operations on the 29th of June 1998. Presently, every atmospheric time step wind fields, air density fields and a gustiness factor are passed from the atmospheric model to the wave model. Then the wave model integrates one time step and determines the two-dimensional wave spectrum. The wave-induced stress is obtained from Eq. (2) which is followed by a determination of the Charnock parameter field. The loop is closed by passing the Charnock field to the atmospheric model which then continues with the next time step.

With this system we have performed a number of impact studies the results of which will be briefly described in the following sections.

2.1 Impact studies: medium-range forecasting.

Initial experiments showed a modest impact of sea-state dependent roughness on atmospheric scores. We illustrate this in Fig. 2 for 28 analyses and 10 day forecasts for the Southern Hemisphere summer time. Shown are anomaly correlation of the 1000 and 500 mb geopotential field. The resolution of the atmospheric model was T_l319 while the wave model had a spatial resolution of $0.5\,\mathrm{deg}$. No impact of this size in the Northern Hemisphere scores were found.

When the two-way interaction of winds and waves was introduced in operations on the 29th of June 1998 there was a pronounced improvement of the quality of the surface wind field. Routinely, first-guess (FG) winds are compared with scatterometer winds (from ERS-2 in this case). As shown in Fig.3 which displays timeseries of bias (ERS-2-FG) and the rms difference, there is a considerable reduction of 10% in the rms error after the introduction of two-way interaction.

However, currently the impact of two-way interaction of wind and waves is more substantial. The main reason for this is an increase of atmospheric resolution from T_l319 to T_l511 (or from 65 to 40 km) which allows for a more real-

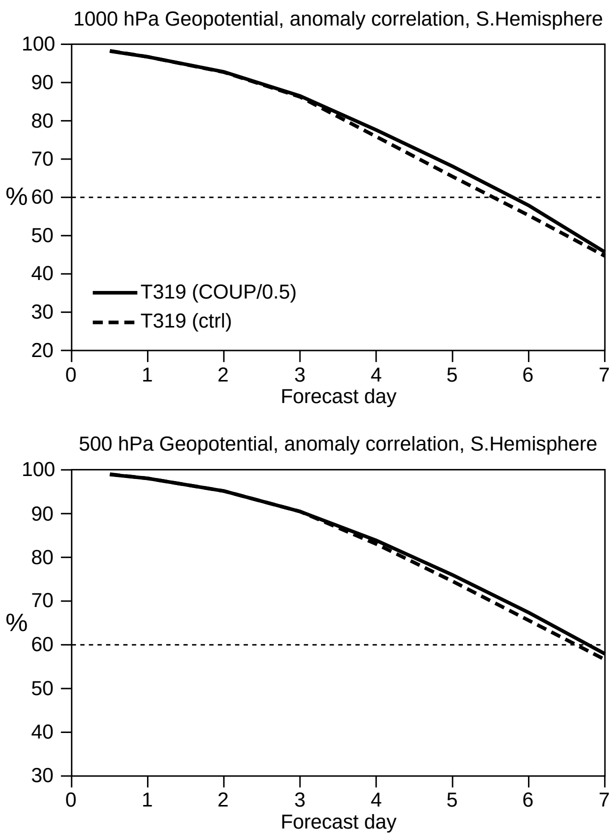

Figure 2: Scores of forecast 1000 and 500 mb geopotential for the Southern Hemisphere for 28 cases in the December 1997-January 1998 period.

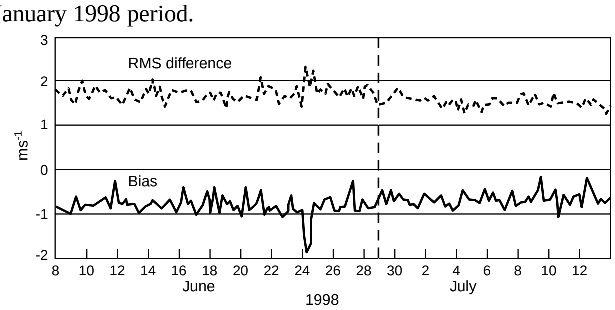

Figure 3: Bias (ERS-2 minus EC FG) and rms difference between the background ECMWF surface winds and the ERS-2 Scatterometer wind measurements.

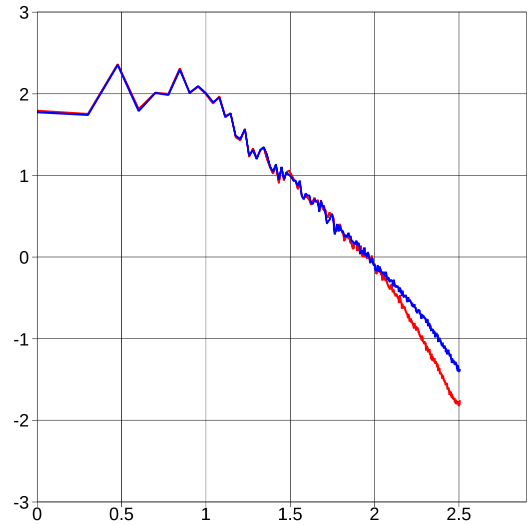

Figure 4: Comparison of surface kinetic energy spectrum as function of total wave number for T_l511 (blue) and T_l319 (red).

istic representation of small spatial scales. It is emphasized that these are the scales that matter for air-sea interaction. That the present atmospheric system has more realistic levels of kinetic energy at the small scales is illustrated by Fig. 4 where we have compared surface kinetic energy spectra from the T_l319 version of the IFS with the T_l511 version. At high wave numbers (small scales) energy levels from the high-resolution model are higher by at least a factor of two.

The more sensitive dependence of the T_l511 version of the IFS on the sea-state dependent drag became evident when we performed experiments with a doubling of angular resolution of the wave spectrum from 12 to 24 directions. Trials with the T_l319 version showed an improvement of forecast skill between 1 and 2 hours. However, when experiments were performed with the T_l511 version of the IFS a substantially larger impact of the increase of angular resolution was found. This is illustrated in Fig. 5 which compares forecast performance in Northern and Southern Hemisphere for 24 cases in August 2000. It is remarked that the sample size is too small to infer general conclusions on the size of the impact, but nevertheless the impact is considerable. Also note, that as a rule of thumb usually larger impact in the summer time is found, presumably because physical processes near the surface play a more important role in the evolution of the weather. In winter time the atmospheric circulation is dominated by baroclinic activity, and physical processes such as surface friction play a relatively minor role, although, there may be a considerable small scale impact in cases of rapidly developing lows (Doyle, 1995; Janssen et al, 2002).

Verification of analysis and forecast. Currently, the coupled IFS-WAM system is used in many applications. For example, in

1) *10-day deterministic forecasts*. Spatial resolution of the atmospheric model is 40 km. Initial conditions for

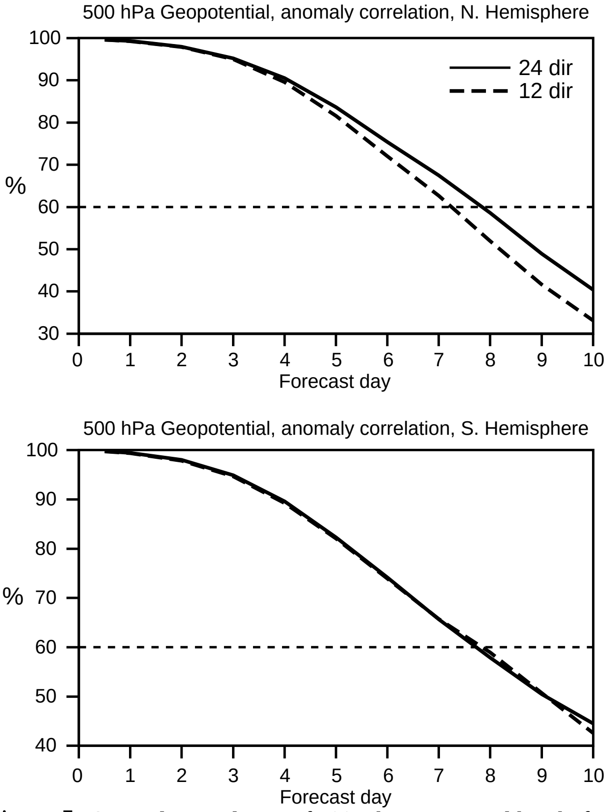

Figure 5: Anomaly correlation of 500 mb geopotential height for the Northern and the Southern Hemisphere for the last 24 days in August 2000. Here, the impact of increased angular resolution on the forecast performance of the T_l511 IFS forecast system is shown.

ocean waves are generated by means of the assimilation of Altimeter wave height data and SAR 2-D spectra from ERS-2. No in-situ buoy observations are assimilated

2) *Ensemble prediction* needed to estimate forecast uncertainty in wind and waves. Spatial resolution of atmospheric model is 80 km. Initial conditions for waves are obtained by means of interpolation of high-resolution wave analysis.

3) *Monthly and Seasonal forecasting*. This is a fairly recent activity at ECMWF. The IFS-WAM model is coupled to the HOPE model in order to take advantage of the predictive skill of the ocean over a timescale of a couple of months. The atmospheric component of the monthly forecast has a spatial resolution of 125 km while for the seasonal forecast the resolution is 210 km.

An important element of any operational forecasting system is its verification against observations. The main verification activities are concentrated on the deterministic medium-range forecast. Analyzed and forecast parameters such as significant wave height and mean period are routinely verified against independent buoy data. A number of operational centers involved in ocean-wave forecasting take part in a project to asses forecast performance against buoy data (Bidlot et al, 2002). However, buoy data are usually only available near coastal areas in the Northern Hemisphere. In order to assess the global performance of the wave prediction system we compare first-guess wave heights against Altimeter wave height, and we compare forecast wave height against the verifying analysis. An overview of these activities is given in Janssen et al (2000). Here we discuss two examples only.

The first example concerns the verification of an analyzed parameter we have not considered before, namely the so-called Stokes transport. This parameter is relevant for studying the impact of ocean waves on the mean circulation. For an infinitely deep ocean it is defined as

$$\vec{T}_{st} = \int_{-\infty}^{0} dz \ \vec{u}_{st},$$

where $\vec{u}_{st}$ is the Stokes drift for a spectrum of waves,

$$\vec{u}_{st} = \frac{2}{g}\int_{0}^{\infty} d\omega \ \omega^3 F(\omega) e^{-2k|z|}, \ k = \omega^2/g.$$

Performing the integration over depth one finds that the Stokes transport is simply given by the first moment of the frequency spectrum,

$$\vec{T}_{st} = \int_{0}^{\infty} d\omega \ \omega F(\omega).$$

Fig. 6 shows a comparison of modelled and observed Stokes transport over a one year period. There is a slight underestimation while the scatter index, defined as the standard deviation of error normalized with the mean of the observations, is about 35%. This is in agreement with the scatter index for significant wave height which on a yearly basis is about 17% nowadays.

By validating model parameters against buoy observations the implicit assumption is being made that the observations are more accurate. Although the observations are of high accuracy and quality-controlled (we have used the off-line products of NDBC) they do not necessarily represent

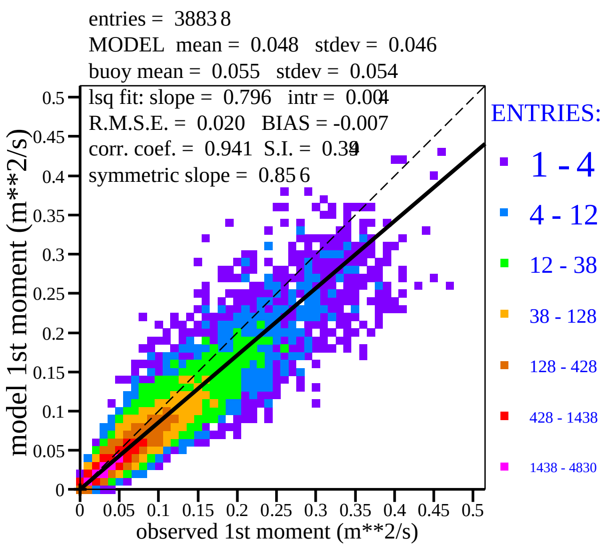

Figure 6: Comparison of analyzed, modelled Stokes transport with buoy data over a one year period. Verification statistics are displayed as well.

the spatial and temporal scales of the forecasting system well. In order to study this we performed a triple collocation study which allows to estimate the "random" error in model, Altimeter and Buoy data, as long as their respective errors are uncorrelated. Fig. 7, which is from Janssen et al (2003), shows the monthly averaged scatter index over a two year period for first-guess, analyzed, ERS-2 Altimeter and buoy wave height. It is clear that the analyzed wave height error is the smallest at the locations where altimeter and buoy data are available. The reason for this is explained in Janssen et al (2003) and is related to the fact that the Optimum Interpolation analysis method has the property that the analysis error is the smaller of the first-guess error and the Altimeter wave height error. The consequence is that the above estimate for the error in the modelled Ekman transport is most likely an overestimate of the 'true' error.

2.2 Impact studies: seasonal integrations.

Janssen and Viterbo (1996) studied the impact of two-way interaction on the seasonal time scale. In order to obtain reliable information on the impact of waves on the atmospheric circulation there is a need for ensemble forecasting, because the variability of the weather, especially over the oceans is high. Therefore 15 coupled and control runs were performed for the winter season of 1990 starting from the analysis of 15 consecutive days. The atmospheric resolution was $T63$, and the wave model had a resolution of $3\,\mathrm{deg}$, while the length of the runs was 120 days. By taking a time average over the last 90 days, followed by an ensemble average a reliable estimate of the mean state of one season could be provided. At the same time, information on the variability may be inferred from the scatter around the mean, and thus a student t-test may be applied to test statistical significance of the mean difference between

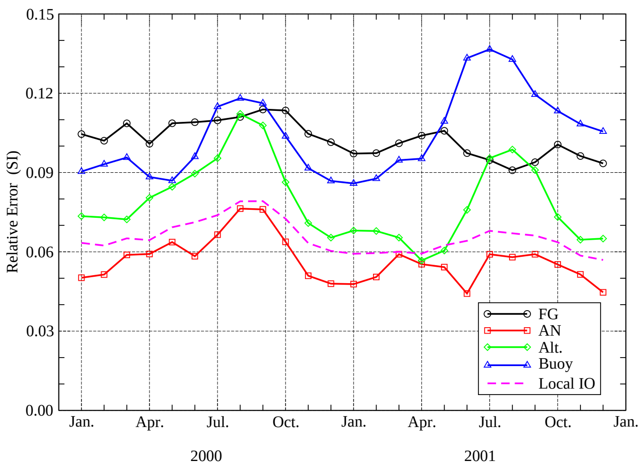

Figure 7: Monthly Relative Error of First-Guess(FG), Analyzed(AN), ERS-2 Altimeter(Alt) and Buoy wave height. Maximum Relative Collocation Difference is 5%. For comparison the Analysis error according to a local Optimum Interpolation(OI) Scheme is shown as well.

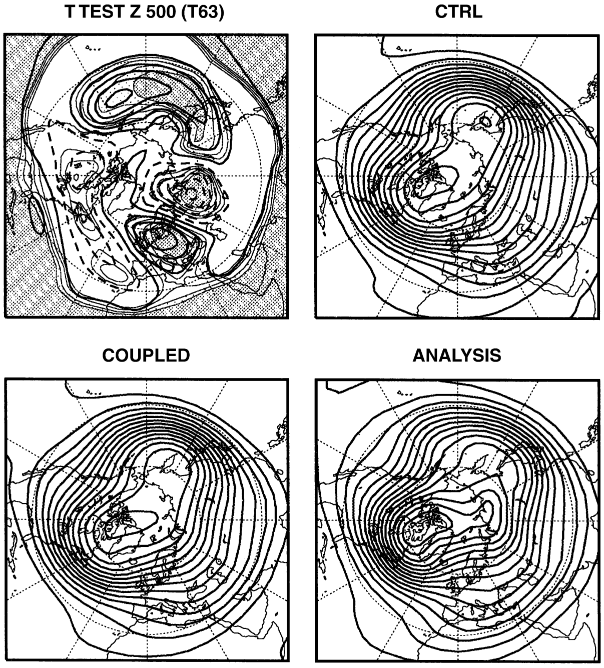

Figure 8: Ensemble mean of coupled and control run and their differences. For comparison the analysed climate is also shown. Period is winter 1990 and area is Northern Hemisphere. The shading indicates a measure of signifi cance. Heavy shading means that there is a probability of 95% that the difference is signifi cant.

ensemble mean of the 500 mb height field and their differences for the Northern Hemisphere, while for comparison purposes we also display the 90-day mean of the corresponding ECMWF analysis. Contours for the mean are plotted every 60 m, while in the difference plot we have indicated by heavy shading the probability of 95% (or more) that the two fields in question are not equal. Significant differences are noted in the storm track areas of the Northern Hemisphere (and, not shown, also for the Southern Hemisphere). We note differences over the Northern Pacific, Europe and Siberia. In the last two areas the coupled climate shows, when compared to the analysis, a considerable improvement. There are also improvements in low-frequency variability over the North Atlantic (not shown).

As far as impact of ocean waves on the atmospheric climate is concerned it should be emphasized that also here resolution of the atmospheric model plays a crucial role. Janssen and Viterbo (1996) also performed seasonal forecasts with the $T21$ version of the coupled system and particularly in the Southern Hemisphere a much reduced impact of the sea-state dependent drag on the atmospheric circulation was found. This should not come as a surprise when it is realized that with $T21$ the mean wind speeds are reduced by as much as 50%, therefore giving a much weaker coupling between wind and waves.

2.3 Impact studies: ocean circulation.

The study by Janssen and Viterbo (1996) also revealed that there were quite large changes in the surface stress in the warm pool area east of Indonesia. Because this area plays a prominent role in understanding certain issues in El Nino prediction, it was thought to be of interest to generate stresses over a one year period in order to investigate the impact of the sea-state dependent momentum transfer on ocean circulation. The long period of one year was thought to be necessary because of the long response times of the ocean circulation.

The stress fields were supplied to Dave Anderson (then at Oxford University) and Gerrit Burgers (KNMI) who forced their tropical ocean model with the coupled and control fluxes. Both models gave considerable differences in the temperature distribution of the surface layer of the ocean (Burgers et al, 1995). An integration period of 6 months gave already a good idea of the kind of impact, which was typically of the order of $1 \deg K$. However, the difference patterns of the two models were surprisingly different. One model showed differences with fairly small spatial scale of the order of 2000 km, while the difference pattern in the other model covered the whole tropical Pacific.

Note that such experiments most likely exaggerate the size of the impact, because there may be an important feedback from the ocean to the atmosphere. The present ECMWF seasonal forecasting system consists of a coupled atmosphere, ocean circulation model. The atmospheric model is coupled to the ocean waves model in two-way interaction mode. Coupling of wind and waves gave a beneficial reduction in the drift in the mean temperature, but the size of the reduction was relatively modest ($0.2 \deg K$ out of a drift of about $1 \deg K$ in 6 months) (T. Stockdale, private communication 2003).

3 TOWARDS A MORE REALISTIC AIR-SEA INTERFACE FOR OCEAN MODELLING.

Ocean waves are the agent that takes care of the momentum and energy transfer from atmosphere to the ocean. Through the process of wave dissipation by, for example white-capping, wave energy is transferred to the ocean column which then generates turbulence and large scale motion of the ocean. It is pointed out that it only makes sense to determine the fluxes through the waves if the circumstances are sufficiently non-stationary or inhomogeneous. If the surface gravity waves were in equilibrium with the wind, the air-sea interface would be transparent, because the energy and momentum received from the wind would be immediately transferred to the ocean column. However, whether unsteadiness and inhomogeneity (or, in other words, wave growth and energy advection) play a role, can only be decided by a determination of these fluxes in actual circumstances. Therefore, the fluxes into the ocean are determined for the month of January 2003 using WAMCy4 forced by operational $10\ m$ wind analyses from ECMWF. In particular, there are considerable deviations from the atmospheric fluxes in the case of the energy flux. This energy flux gives rise to large deviations from the balance of production and dissipation of kinetic energy. An appropriate turbulence scheme to deal with such circumstances is a scheme developed by Mellor and Yamada (1982). In case of neutral stratification and no Coriolis force an exact solution for kinetic energy and current profile is found. We extend the Mellor-Yamada scheme by modelling the effects of wave breaking via the divergence of the correlation between pressure and vertical velocity. This idea is similar in spirit as found in Janssen (1999) who argued that because of growing waves by wind the corresponding term in air may be important.

However, first we comment extensively on the problem of the interaction of the mean flow and surface gravity waves. This is followed by a discussion on the need to include ocean currents in the determination of the atmospheric-ocean fluxes, and to provide the proper boundary condition for the atmospheric flow.

3.1 Ocean waves, the surface jet and ocean circulation.

In the usual description of the ocean the momentum of the ocean waves is not taken into account, despite the fact that a considerable list of authors (Hasselmann, 1970; Weber, 1983; Jenkins, 1987a; Xu and Bowen, 1994; McWilliams and Restrepo, 1999) have pointed out that in a rotating ocean the ocean waves excert a wave-induced stress on the Eulerian mean flow which results in a force equal to $\vec{u}_s \times \vec{f}$, where $\vec{f}$ is the Coriolis parameter, and $\vec{u}_s$ equals the Stokes drift. This additional force has a considerable impact on the Ekman turning of the surface current (Weber, 1983; Jenkins, 1987b; Polton et al, 2003). Here, we reconsider the problem of wave, mean-flow interaction in two ways. First, this problem is discussed in the context of the conservation law of total column momentum. Second, we study the momentum balance in detail by means of the simple example suggested by Xu and Bowen (1994). A treatment will be given that starts from the general case of internal gravity waves, and the case of surface gravity waves follows by an appropriate choice of the equilibrium density profile. As a result we find that in addition to the usual $\vec{u}_s \times \vec{f}$ force a highly localized surface drift needs to be included in the Coriolis force as well. The transport associated with the surface drift exactly cancels the transport by the Stokes drift with the consequence that ocean waves do not affect the Ekman transport.

Conservation of total mass and momentum. Consider an incompressible fluid (water) in a constant gravitational field on a rotating earth. Let the body of water with air above it be of infinite extent in the horizontal while in the vertical it extends from $z = -D$ (with D the water depth) to $z = \eta$, with $\eta(x,y,t)$ the unknown surface elevation. Let us assume that the water motion is governed by the continuity equation

$$\frac{\partial}{\partial t}\rho + \nabla.(\rho\vec{u}) = 0. \quad (5)$$

and the momentum equation

$$\frac{\partial}{\partial t}\rho\vec{u} + \nabla.\rho\vec{u}\vec{u} = -\nabla p + \rho\vec{g} + \rho\vec{u}\times\vec{f}. \quad (6)$$

These equations apply to the domain $-D < z < \eta$ and the boundary conditions are

$$z = \eta(x,y,t):\ \frac{\partial}{\partial t}\eta + \vec{u}.\nabla_h\eta = w,\ p = p_a, \quad (7)$$

where p_a is the given air pressure at the sea surface and $\nabla_h = (\partial/\partial x, \partial/\partial y)$ is the horizontal gradient operator. At the flat bottom $D = D_0$ we impose the condition that no fluid penetrates the bottom

$$z = -D:\ w = 0. \quad (8)$$

Following Longuet-Higgins and Stewart (1961), Whitham (1962), and Phillips (1977) conservation laws for the mean surface elevation ζ and the mean horizontal velocity $\vec{U}$ may now be obtained by integration of the continuity equation and the momentum equation over the depth of the water, followed by a suitable ensemble averaging. The ensemble average $\langle . \rangle$ is supposed to filter the linear gravity wave motion. Here, the mean surface elevation ζ is defined as

$$\zeta = \langle\eta\rangle, \quad (9)$$

while the mean horizontal velocity $\vec{U}$ follows from

$$\vec{U} = \frac{\vec{P}}{\rho h}, \quad (10)$$

with $h = D + \zeta$ the slowly varying water depth. Note that $\vec{P}$ is the *total* mass flux

$$\vec{P} = \langle\int_{-D}^{\eta} dz\ \rho\vec{u}\rangle, \quad (11)$$

i.e., it consists of the sum of the water column mean $\vec{P}^m$ and the surface layer mean $\vec{P}^w$, defined as (Hasselmann, 1971)

$$\vec{P}^m = \langle\int_{-D}^{\zeta} dz\ \rho\vec{u}\rangle,\ \ \vec{P}^w = \langle\int_{\zeta}^{\eta} dz\ \rho\vec{u}\rangle. \quad (12)$$

In the linear approximation the surface layer mean mass flux may be expressed in terms of the wave momentum

$$\vec{P}^w = \rho g\int d\vec{k}\ \vec{l}\ F/c, \quad (13)$$

where c is the phase speed of the gravity waves and $\vec{l} = \vec{k}/k$ is a unit vector pointing in the direction of the wave propagation. As a consequence, the mean horizontal velocity $\vec{U}$ is the sum of the ocean circulation velocity $\vec{U}_c$ and the wave-induced drift $\vec{U}_{surf}$,

$$\vec{U} = \vec{U}_c + \vec{U}_{surf}. \quad (14)$$

Note that the momentum in the mean surface drift equals the one of the Stokes drift.

The conservation laws become (Mastenbroek et al, 1993)

$$\frac{\partial}{\partial t}\zeta + \nabla_h.\left(h\vec{U}\right) = 0, \quad (15)$$

and

$$\begin{aligned}\left(\frac{\partial}{\partial t} + \vec{U}.\nabla_h\right)\vec{U} \quad &+ \quad g\nabla_h\zeta + \frac{1}{\rho}\nabla_h p_a \\ = \vec{U}\times\vec{f} \quad &+ \quad \frac{\vec{\tau}_a - \vec{\tau}_b}{\rho h} - \frac{1}{\rho h}\nabla_h.\mathsf{S}, \quad (16)\end{aligned}$$

where $\vec{\tau}_a$ and $\vec{\tau}_b$ represent the atmospheric surface stress and the bottom stress. The radiation stress tensor S represents the contribution of the wave motions to the mean horizontal flux of horizontal momentum. In terms of the wave spectrum it is given by

$$S_{ij} = \rho g\int d\vec{k}\left\{\frac{v_g}{c}l_i l_j + \left(\frac{v_g}{c} - \frac{1}{2}\right)\delta_{ij}\right\}F(\vec{k}). \quad (17)$$

Note that the first term corresponds to advection of wave momentum, while the second term consists of a combination of contributions from the wave-induced pressure and the wave-induced stress (Phillips, 1977).

As pointed out by Whitham (1974) the momentum conservation law (16) assumes its most simple form when the mass transport velocity including the wave momentum is used. In this formulation of the conservation laws, ocean waves only appear explicitely through the radiation stress tensor S. Implicitely it also appears through parametrizations of the stress. For example, in case the bottom stress $\vec{\tau}_b$ is modelled in terms of the current velocity $\vec{U}_c$ rather than the total velocity $\vec{U}$. Mastenbroek et al (1993) parametrized the bottom stress in terms of the total velocity and used the above depth-averaged equations in a study of the impact of sea-state dependent atmospheric stress on a number of storm surges in the North Sea. In particular for rapidly varying atmospheric lows a considerable increase in atmospheric stress was found. This resulted in increases of the storm surge at several stations along the English and Dutch coasts of the order of $30\ cm$ and a good agreement with observed water levels was found. These authors also studied the importance of the radiation stress. In one case the water levels showed an increase of $10-15\ cm$ when the radiation stress was included in the calculation, while in two other cases the impact was less than $5\ cm$. The effect of the radiation stress, therefore, cannot always be neglected, especially when shallow water effects are important.

Although the depth-averaged continuity and momentum equations show their simplest form in terms of the total velocity, there is a definite need to know the ocean circulation velocity $\vec{U}_c$. This can be obtained in two ways. First, one could simply subtract the surface drift from the total velocity. Secondly, following Hasselmann (1971) one could obtain the corresponding evolution equations for the current velocity $\vec{U}_c$. To that end one eliminates from (16) the rate of change in time of the wave momentum by means of the energy balance equation (1). Dividing the energy balance equation by the phase speed and integration over wavenumber $\vec{k}$ gives

$$\begin{aligned} \frac{\partial}{\partial t}\vec{P}^w &= -\rho g \nabla . \int d\vec{k}\, \frac{\vec{l}\vec{v}_g}{c}\, F \\ &+ \rho g \int \frac{d\vec{k}}{c}\, \left(S_{in} + S_{nl} + S_{diss} + S_{bot}\right). \end{aligned} \quad (18)$$

Substitution of (18) into (16) gives the following evolution equation for the ocean circulation velocity $\vec{U}_c$

$$\left(\frac{\partial}{\partial t} + \vec{U}_c.\nabla_h\right)\vec{U}_c + g\nabla_h\zeta + \frac{1}{\rho}\nabla_h p_a = \vec{U}_c \times \vec{f}$$
$$+\vec{U}_{surf} \times \vec{f} + \frac{\vec{\tau}_{oc,a} - \vec{\tau}_{oc,b}}{\rho h} - \frac{1}{\rho h}\nabla_h.\mathsf{T}. \quad (19)$$

and it is straightforward to rewrite the continuity equation:

$$\frac{\partial}{\partial t}\zeta + \nabla_h.\left(h\vec{U}_c\right) = -\nabla_h.\left(h\vec{U}_{surf}\right). \quad (20)$$

The conservation laws for the mean ocean circulation differ in a number of respects from the laws for the total current. First, the continuity equation now shows an explicit dependence on the mass flux related to the ocean waves. Second, in the momentum equation effects of the advection of wave momentum have been eliminated, therefore, $v\mathsf{T}$ becomes

$$T_{ij} = \rho g \int d\vec{k}\left(\frac{v_g}{c} - \frac{1}{2}\right)\delta_{ij} F(\vec{k}). \quad (21)$$

Third, the surface stress and the bottom stress are modified accordingly. For example, the surface stress felt by the mean circulation is the total stress minus the net stress going into the waves, or,

$$\vec{\tau}_{oc,a} = \vec{\tau}_a - \rho g \int \frac{d\vec{k}}{c}\, \left(S_{in} + S_{nl} + S_{diss}\right), \quad (22)$$

and the bottom stress becomes

$$\vec{\tau}_{oc,b} = \vec{\tau}_b + \rho g \int \frac{d\vec{k}}{c}\, S_{bot}, \quad (23)$$

Fourth, the wave momentum equation (18) does not involve an explicit Coriolis term, and therefore the mean circulation experiences an additional force given by $\rho\vec{U}_{surf} \times \vec{f}$. It is this additional force, which recently has been given considerable attention.

It is important to note that the structure of the equations for the mean horizontal velocity $\vec{U}$ and the ocean circulation velocity $\vec{U}_c$ are similar, but that there are detailed differences. Nevertheless, since one follows from the other these two alternative formulations should give the same information on for example the mean surface elevation ζ. However, following Mastenbroek et al (1993), there is, because of its simplicity, a slight preference to use in numerical studies of the interaction of ocean waves and ocean circulation the momentum equations in terms of the total horizontal velocity $\vec{U}$, Eqns. (15) and (16).

Despite our preference, we will study in the context of the mean circulation equations the impact of ocean waves as well, by, for example, determining the difference between the atmospheric stress $\vec{\tau}_a$ and the stress felt by the mean ocean circulation $\vec{\tau}_{oc,a}$ (cf. Eq. (22)).

Nevertheless, even in the context of the evolution equations for the total horizontal velocity, a number of issues need to be adressed. The first one is how to parametrize the turbulent fluxes. In the following sections it will be shown that there is large difference in the Ekman spiral depending on whether one uses the total velocity $\vec{U}$ in the turbulent stress or the ocean circulation velocity $\vec{U}_c$. Also, it is found that the surface drift $\vec{U}_{surf}$ is highly concentrated near the surface of the ocean. Therefore, the surface velocity really differs from the mean velocity of the surface layer, and this difference may have consequences for the determination of the atmosphere-ocean fluxes. In other words, near the surface it is of interest to study the vertical profile of the total velocity.

The surface drift. Consider a single gravity wave at the interface of air and water. Suppose the surface elevation is given by

$$\eta = a\cos\theta,\ \theta = kx - \omega t, \quad (24)$$

hence, we take a wave with amplitude a, wavenumber k and angular frequency ω which is propagating to the right. The question now is what is in a Eulerian frame the mean momentum as function of height z. Clearly, since this is a periodic wave there is no mean momentum below $z = -a$ or above $z = a$, hence only mean momentum for $|z| < a$ will be found.

The mean momentum at height z is

$$\begin{aligned} P &= \frac{1}{2\pi}\int_0^{2\pi} d\theta\ \rho u \\ &= \frac{\rho_w}{2\pi}\int_{-\theta_0}^{\theta_0} d\theta\ u_w + \frac{\rho_a}{2\pi}\int_{\theta_0}^{2\pi-\theta_0} d\theta\ u_a, \end{aligned} \quad (25)$$

where θ_0 follows from

$$z = a\cos\theta,$$

hence

$$\theta_0 = \arccos(z/a). \quad (26)$$

Here, the subscripts a and w refer to air and water, respectively. For simplicity we assume potential flow $u = \partial\phi/\partial x = k\partial\phi/\partial\theta$ where

$$\begin{aligned} \phi_w &= +cae^{kz}\sin\theta,\ c = \omega/k \\ \phi_a &= -cae^{-kz}\sin\theta \end{aligned} \quad (27)$$

(Note that across the interface the u component of the velocity jumps, while the vertical component is continuous), and the mean momentum becomes

$$P = \frac{\rho_a + \rho_w}{\pi} k\phi(\theta_0),$$

or,

$$P = \frac{\omega a}{\pi}(\rho_a + \rho_w)\sin\theta_0, \tag{28}$$

where we ignore the $\exp(-k|z|)$ factor because we take weakly nonlinear waves, hence, $ka \ll 1$.

Now, $\sin\theta_0 = \sqrt{1-\cos^2\theta_0} = \sqrt{1-(z/a)^2}$, and therefore the height dependence of the mean momentum follows from

$$P = \frac{1}{2}(\rho_a + \rho_w)\omega a^2 d(z,a), \tag{29}$$

where for small amplitude a the function $d(z,a)$ is highly localized around $z = 0$,

$$d(z,a) = \frac{2}{\pi a}\sqrt{1-\left(\frac{z}{a}\right)^2}, \tag{30}$$

which is normalized to 1, ie. $\int dz\; d(z,a) = 1$. In particular in the limit $a \to 0$ the function $d(z,a)$ behaves like a δ-function and hence the surface drift becomes a surface jet:

$$\lim_{a\to 0} P \to \frac{1}{2}(\rho_a + \rho_w)\omega a^2 \delta(z), \tag{31}$$

and one would expect that such a highly singular jet, which has the same momentum as the Stokes drift, should play a role in the mean momentum equations.

Note that, although linear theory gives an explosion for the surface drift at $z = 0$, the present consideration gives a definite answer. From (29) one finds

$$P(z=0) = \frac{\rho_a + \rho_w}{\pi}\omega a \tag{32}$$

Eq. (32) reflects the singular nature of the surface drift as well. Normally, one expects that such a drift is of second order in the amplitude a, but the present consideration suggests that at the surface the drift is $\mathcal{O}(a)$. Remarkebly, with a steepness $ka = 0.1$ the drift is $\sim 3\%$ of the phase speed of the wave.

Wave, mean-flow interaction and the surface drift. We present here a derivation of the mean flow equations that treats air and water on an equal footing, by considering the case of stable, general density profiles. Only at the end of the analysis the appropriate density profiles are specified.

Starting point are the equations for an adiabatic fluid on a rotating earth, and we consider phenomena with a speed much smaller than the sound speed, hence

$$\begin{aligned} \nabla.\vec{u} &= 0, \\ \frac{\partial}{\partial t}\rho\vec{u} + \nabla.\rho\vec{u}\vec{u} &= -\nabla p + \rho\vec{g} + \rho\vec{u}\times\vec{f}, \\ \left(\frac{\partial}{\partial t} + \vec{u}.\nabla\right)\rho &= 0. \end{aligned} \tag{33}$$

The equilibrium is given by

$$\begin{aligned} \vec{u}_0 = 0,\ \vec{g} &= -g\hat{e}_z, \\ \rho_0 = \rho_0(z), p_0 = p(z) &= -g\int dz\;\rho_0(z) \end{aligned} \tag{34}$$

First we shall apply linear theory, which enables us to obtain the necessary fluxes in the mean flow equations. The resulting fluxes will induce a mean flow, but we shall assume that the waves are much faster than the mean flow. In other words, mean flow effects on the waves can be ignored.

Consider a plane wave propagating in the x-direction so there is no y-dependence. The perturbations are assumed to have the form

$$\begin{aligned} (\delta\rho, \delta u, \delta v, \delta w, \delta p) &= (\hat{\rho}, \hat{u}, \hat{v}, \hat{w}, \hat{p})\, e^{i\theta} + c.c,\ \theta \\ &= kx - \omega t, \end{aligned} \tag{35}$$

where the amplitudes are still functions of height z. Linearizing Eq. (33) around the equilibrium (34) then gives

$$\begin{aligned} ik\hat{u} + \hat{w}' &= 0, \\ i\omega\hat{u} &= ik\hat{p}/\rho_0 - f\hat{v}, \\ i\omega\hat{v} &= f\hat{u}, \\ i\omega\hat{w} &= g\hat{\rho}/\rho_0 + \hat{p}'/\rho_0, \\ i\omega\hat{\rho} &= \hat{w}\rho_0', \end{aligned} \tag{36}$$

where a prime denotes differentiation with respect to z.

Combining the first and third equation of (36) we have

$$\hat{v} = \frac{f\hat{w}'}{\omega k},\ \hat{u} = -\frac{\hat{w}'}{ik} \tag{37}$$

hence cross velocity and vertical velocity are in phase, giving a non-zero flux $\rho_0\langle\delta v\delta w\rangle$ which produces a force orthogonal to the wave propagation direction.

The density perturbation becomes

$$\hat{\rho} = \rho_0'\frac{\hat{w}}{i\omega} \tag{38}$$

while from the second equation of (36) the pressure perturbation becomes

$$\hat{p} = i\frac{\omega}{k^2}\rho_0 D\hat{w}',\ D = 1 - (f/\omega)^2. \tag{39}$$

Note that in practice for surface gravity waves $f \ll \omega$, hence $D \to 1$.

Finally, eliminating pressure and density perturbation from the fourth equation of (36) we arrive at the Sturm-Liouville type of differential equation

$$\frac{d}{dz}\left(\rho_0\frac{d}{dz}\hat{w}\right) = \frac{\kappa^2\hat{w}}{\omega^2}\left(g\rho_0' + \omega^2\rho_0\right), \tag{40}$$

where $\kappa^2 = k^2/D$, and the boundary conditions are the vanishing of the vertical velocity at infinity:

$$\hat{w} \to 0 \text{ for } |z| \to \infty. \tag{41}$$

We do not use the so-called Boussinesq approximation (ignore all density variations except in combination with acceleration of gravity) because, in particular for surface gravity waves the density gradient is large.

Some general properties of the boundary value problem (40), (41) are presented now. First, it is shown that for stable density profiles the gravity waves are stable. As a consequence, the flux $\rho_0\langle\delta u\delta w\rangle$ vanishes. Only when the waves are slightly growing or damped will the stress in the wave direction be finite. The result is a force which is proportional to the time derivative of the amplitude of the waves (see also Andrews and McIntyre, 1976). We also obtain a general expression for the cross force $\partial\rho_0\langle\delta v\delta w\rangle/\partial z$. In the special case of surface gravity waves this force will give rise to a singular contribution proportional to $\delta(z)$.

The dispersion relation is obtained from (40) by multiplication with $\hat{w}^*$ and integration of the result from $z \to -\infty$ to $z \to +\infty$. Partial integration of the LHS, and making use of the boundary condition for $\hat{w}$ gives

$$\begin{aligned}\omega^2 \int_{-\infty}^{\infty} dz\ \rho_0 \left\{|\hat{w}'|^2 + \kappa^2|\hat{w}|^2\right\} \\ = -g\kappa^2 \int_{-\infty}^{\infty} dz\ \rho_0'|\hat{w}|^2 \end{aligned} \tag{42}$$

Considering only the case of high-frequency waves, such as surface gravity waves are, we ignore f with respect to ω in κ. Then, if the density profile is stable ($\rho_0' < 0$) we have real solutions for angular frequency ω, a result which is well-known.

Next, we will derive some general expressions for the relevant fluxes. First, consider the stress along the wave direction,

$$\tau_{uw} = -\rho_0\langle\delta u\delta w\rangle = -\rho_0\left(\hat{u}\hat{w}^* + c.c\right) \tag{43}$$

Using (37) one finds

$$\tau_{uw} = \frac{\mathcal{W}}{k} \tag{44}$$

where $\mathcal{W}$ is the Wronskian of the differential equation (40),

$$\mathcal{W} = -i\rho_0\left(\hat{w}'\hat{w}^* - \hat{w}^{*'}\hat{w}\right). \tag{45}$$

If there are no critical layers the Wronskian is constant. This follows immediately by differentiating $\mathcal{W}$ with respect to z, and using (40)

$$\frac{d}{dz}\mathcal{W} = -i\kappa^2|\hat{w}|^2\left(\frac{g\rho_0'}{\omega^2} + \rho_0\right) + c.c, \tag{46}$$

and this vanishes because for real ω the term in brackets is real. Hence, τ_{uw} is constant and since $\hat{w}$ vanishes for large heights we conclude that τ_{uw} vanishes.

Remark that the vanishing of τ_{uw} depends on ω being real. In unsteady circumstances there will be a finite stress. Unsteadiness can be mimicked by introduction of a slight damping in the system of equations. In Eqns. (33) we replace

$$\frac{\partial}{\partial t} \to \frac{\partial}{\partial t} + \epsilon \tag{47}$$

everywhere, where ϵ is a small damping rate. This effectively means that angular frequency ω is replaced by $\omega - i\epsilon$. For complex frequency the right-hand side of (46) does not vanish. As a consequence one finds as force along the wave

$$\frac{\partial}{\partial z}\tau_{uw} = -2\frac{gk}{\omega^2}\rho_0'\frac{1}{\omega}\frac{\partial}{\partial t}|\hat{w}|^2, \tag{48}$$

hence the force is proportional to the time derivative of the vertical velocity (cf. Andrews and McIntyre, 1976). Note that for surface gravity waves, when the density shows a jump at $z = 0$, the above force is singular. It should be clear, however, that there may be several causes why ocean wave energy changes with time, and in general the stress τ_{uw} depends in a complicated fashion on e.g. the wind profile in air (cf. Komen et al, 1994). For simplicity it will be assumed from now on that the sea state is steady, hence τ_{uw} vanishes.

The next flux of interest is

$$\tau_{vw} = -\rho_0\langle\delta v\delta w\rangle = -\rho_0(\hat{v}^*\hat{w} + c.c) \tag{49}$$

Using (37) this may be written as

$$\tau_{vw} = -\frac{f}{\omega k}\left(\rho_0\hat{w}^*\hat{w}' + c.c.\right). \tag{50}$$

Differentiating the stress with height and making use of the differential equation for $\hat{w}$ gives the important relation

$$\begin{aligned}\frac{\partial}{\partial z}\tau_{vw} = & - \frac{f}{\omega k}\left\{\rho_0\left[\kappa^2|\hat{w}|^2 + |\hat{w}'|^2\right] + \frac{g\kappa^2}{\omega^2}\rho_0'|\hat{w}|^2\right\} \\ & + c.c.\ . \end{aligned} \tag{51}$$

The force given in Eq. (51) consists of two parts. The first part is given by the term in square brackets and is a regular function of height, because, although $\hat{w}'$ may show a jump at the air-sea interface, $|\hat{w}'|^2$ is continuous. For the water wave problem this will give rise to the $\vec{u}_s \times \vec{f}$-force. The second part is proportional to the density gradient. This part is, however, of a special nature because for the air-water problem ρ_0 shows a jump, hence $\rho_0' \sim \delta(z)$. Therefore, there is a very important contribution of the force very close to the surface. This force has, as far as we know, never been mentioned in the literature. It is important to retain this $\delta(z)$-force, however, because of momentum conservation.

In order to show that the force $\partial\tau_{vw}/\partial z$ conserves total momentum one needs to show that

$$\int_{-\infty}^{\infty} dz\ \frac{\partial}{\partial z}\tau_{vw} = 0. \tag{52}$$

This follows immediately from integration of Eq.(51) over height and making use of the dispersion relation (42).

The special case of surface gravity waves. Let us now consider the special case of surface gravity waves by taking as density profile

$$\rho_0 = \begin{cases} \rho_a, \ z > 0, \\ \\ \rho_w, \ z < 0. \end{cases} \quad (53)$$

where ρ_a and ρ_w are constants. The density ratio $\epsilon = \rho_a/\rho_w$ is assumed to be small.

In air and water the problem simplifies considerably because there is no density gradient. From (40) the relevant equation for the amplitude of the vertical velocity becomes

$$\frac{d^2}{dz^2}\hat{w} = \kappa^2 \hat{w}.$$

Taking the boundary condition of vanishing vertical velocity at infinity into account we have

$$\hat{w} = \hat{w}_0 e^{-\kappa|z|}. \quad (54)$$

The vertical velocity amplitude $\hat{w}_0$ is connected to the surface elevation amplitude $\hat{\eta}$ in the usual manner

$$\frac{\partial \eta}{\partial t} = w \ \Rightarrow \ \hat{w}_0 = -i\omega\hat{\eta}. \quad (55)$$

The dispersion relation for ω may be obtained from the jump-condition at the interface (Komen et al, 1994). Alternatively, one simply substitutes the solution (54) together with the density profile (53) into the general dispersion relation (42). The eventual result is

$$\omega^2 = g\kappa \frac{1-\epsilon}{1+\epsilon} \quad (56)$$

The force (51) can now readily be evaluated. It becomes

$$\frac{\partial}{\partial z}\tau_{vw} = -f\rho_0 \left(u_{stokes} - u_{surf}\right) \quad (57)$$

where

$$\rho_0 u_{surf} = 2\left(\rho_a + \rho_w\right)\delta(z)\omega|\hat{\eta}|^2, \quad (58)$$

while

$$u_{stokes} = 4\omega k|\hat{\eta}|^2 e^{-2k|z|}. \quad (59)$$

Here, we approximated κ by k ($f/\omega \ll 1$). With the identification $2\hat{\eta} \rightarrow a$ the surface momentum in (58) is found to be identical to the mean momentum (31) from the simple considerations given in section 3.1.1.

Note that the result (57) can also be obtained directly from the substitution of the solution for $\hat{w}$ into the expression for the stress (49). This gives

$$\tau_{vw} = 2\rho_0 f\omega|\hat{\eta}|^2 e^{-2k|z|} sign(z) \quad (60)$$

and the stress profile is depicted in the Fig. 9. The jump in the stress τ_{vw} at the interface of air and water is caused by the discontinuity of the fluctuating horizontal velocity.

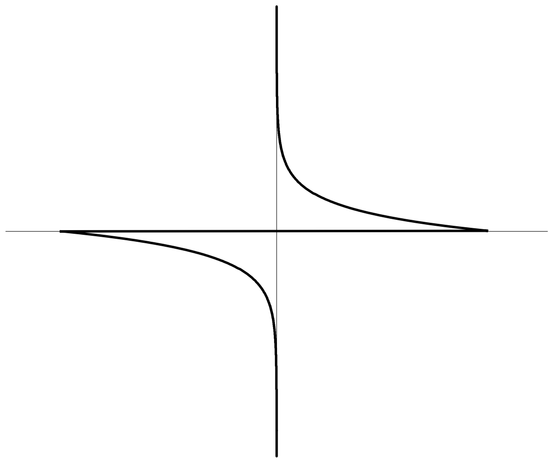

Figure 9: Profile of cross-stress τ_{vw}. For display purposes air and water density are equal.

According to (60) $\tau_{vw}(0) = 0$ and differentiation of (60) with respect to z gives (57). There is no contribution from the derivative of the density ρ_0 because of the vanishing of the wave stress τ_{vw} at the surface. This condition is quite important because it implies that in each fluid momentum is conserved by the $\partial\tau_{vw}/\partial z$ - force.

Other fluxes in the mean flow equations, such as $\langle\delta\rho\delta w\rangle$, $\langle\delta\rho\delta v\rangle$ and $\langle\delta\rho\delta u\rangle$ can be shown to vanish. The first two fluxes vanish because δv and δw are out of phase with $\delta\rho$. For the flux in the x-direction one finds

$$\langle\delta\rho\delta u\rangle = 2\rho_0'\omega|\hat{\eta}|^2 sign(z) e^{-2k|z|},$$

and this vanishes for the same reason as the vanishing of τ_{vw} at the surface, namely $sign(z)\rho_0' = 0$ at $z = 0$.

Mean-flow equations. We first consider the horizontal components of the momentum equations. They read

$$\begin{aligned} \frac{\partial}{\partial t}\rho u + \frac{\partial}{\partial x}\rho u^2 + \frac{\partial}{\partial z}\rho uw &= -\frac{\partial}{\partial x}p + \rho f v \\ \frac{\partial}{\partial t}\rho v + \frac{\partial}{\partial x}\rho uv + \frac{\partial}{\partial z}\rho vw &= -\rho f u \end{aligned} \quad (61)$$

Next, one writes the relevant quantities as the sum of a mean value and a fluctuating part

$$\rho = \rho_0 + \delta\rho, \ u = u_0 + \delta u, \ v = v_0 + \delta v, \ w = \delta w, \quad (62)$$

hence the ensemble average of the fluctuations, e.g. $\langle\delta u\rangle$ vanishes. Taking the ensemble average of (61), ignoring third moments and using the vanishing of the density fluxes gives

$$\begin{aligned} \frac{\partial}{\partial t}\rho_0 u_0 + \frac{\partial}{\partial z}\rho_0\langle\delta u\delta w\rangle &= f\rho_0 v_0 \\ \frac{\partial}{\partial t}\rho_0 v_0 + \frac{\partial}{\partial z}\rho_0\langle\delta v\delta w\rangle &= -f\rho_0 u_0 \end{aligned} \quad (63)$$

Making use of the expressions for the fluxes, i.e. vanishing τ_{uw} because of steadiness and (57) the final result becomes

$$\begin{aligned} \frac{\partial}{\partial t}\rho_0 u_0 &= f\rho_0 v_0 \\ \frac{\partial}{\partial t}\rho_0 v_0 &= -f\left[\rho_0(u_0 - u_{surf}) + \rho_0 u_{stokes}\right] \end{aligned} \quad (64)$$

It is clear that we are dealing here with forced inertial oscillations. In the steady state one finds

$$\rho_0 u_0 = \rho_0 (u_{surf} - u_{stokes}),\ \rho_0 v_0 = 0, \tag{65}$$

therefore, we obtain the curious result that a steady state is achieved which is independent of the size of the Coriolis parameter f.

The surface current consists of two terms. The second one is the negative of the Stokes drift, while the first term is new (at least in the surface gravity wave context) and is highly singular. Let us call this contribution the surface drift. This drift formally explodes at the surface but it has nevertheless a finite total momentum which exactly equals the total momentum in the Stokes drift (as can easily be verified). Hence,

$$\int_{-\infty}^{\infty} dz\ \rho_0 u_0 = 0,$$

in agreement with the momentum conservation relation (52).

Note that the generalization of these results to the case of many waves is immediate. Simply replace $|\hat{\eta}|^2$ by $F(\omega)/2$ with $F(\omega)$ the wave spectrum and integrate over ω. The surface and the Stokes drift become

$$\rho_0 u_{surf} = (\rho_a + \rho_w)\delta(z) \int_0^{\infty} d\omega\ \omega F(\omega),$$

$$\rho_0 u_{stokes} = \frac{2}{g}\rho_0 \int_0^{\infty} d\omega\ \omega^3 F(\omega) e^{-2k|z|},\ k = \omega^2/g. \tag{66}$$

Let us finally consider the mean vertical momentum balance. First, from incompressibility it follows that the mean vertical velocity vanishes. Ensemble averaging then gives

$$\frac{\partial}{\partial z}\rho_0 \langle \delta w^2 \rangle = -\frac{\partial}{\partial z}\langle p \rangle - \rho g \tag{67}$$

Apart from a constant the mean pressure becomes

$$\langle p \rangle = -\rho_0 \langle \delta w^2 \rangle - g \int dz\ \rho_0 \tag{68}$$

It should be noted that ocean waves give a considerable contribution to the water pressure near the air-sea interface. The variance in vertical velocity can be related to the wave spectrum according to

$$\langle \delta w^2 \rangle = \int_0^{\infty} d\omega\ \omega^2 F(\omega) e^{-2k|z|}. \tag{69}$$

Using a simple parametrisation for the wave spectrum,

$$F = \alpha_p g^2 \omega^{-5},\ \omega > \omega_p,$$

one finds

$$\langle \delta w^2 \rangle\big|_{z=0} = \frac{\alpha_p}{2}\left(\frac{g}{\omega_p}\right)^2.$$

With $\alpha_p = 0.01$ and a peak phase speed g/ω_p of 10 m/s this gives a contribution of 5 mb to the surface pressure.

Consequences for ocean circulation. Generalizing (64) to the case of arbitrary wave propagation direction, and adding the effects of turbulent momentum transport through the divergence of a turbulent stress $\vec{\tau}_{turb}$ one finds

$$\frac{\partial}{\partial t}\rho \vec{u} = \rho\left(\vec{u} - \vec{u}_{surf}\right) \times \vec{f} \quad + \quad \rho \vec{u}_{stokes} \times \vec{f} \quad + \quad \frac{\partial}{\partial z}\vec{\tau}_{turb} \tag{70}$$

Denoting the surface stress by $\vec{\tau}_0$ and assuming that the turbulent stress vanishes for large depth, one then finds in the steady state for the Ekman transport

$$\vec{T}_E = \int_{-\infty}^{0} dz\ \rho \vec{u} \tag{71}$$

the result

$$\vec{T}_E = \frac{\vec{\tau}_0 \times \vec{f}}{f^2}, \tag{72}$$

because the total momentum in the surface drift cancels the momentum in the Stokes drift. Therefore, the classical result for the Ekman layer follows. Omitting the surface drift would imply considerable deviations from this classical result, up to 50% or more in the polar regions.

The above discussion would perhaps leave the impression that, as there is no impact on the Ekman transport, the Stokes drift would not affect ocean circulation. However, it will turn out that the impact of the ocean waves on the circulations depends in a crucial way on how the interaction between the surface drift and water turbulence is modelled.

In order to see this, let us model water turbulence by means of a simple mixing length model. A discussion on more sophisticated models, such as the Mellor-Yamada (1982) scheme is given at the end of this paper. Thus, we assume that the turbulent momentum diffusion can be modelled with a constant eddy viscosity. In addition, we assume that the ocean waves are propagating in the x-direction. Introducing the complex velocity W according to

$$W = u + iv, \tag{73}$$

and writing for the turbulent stress

$$\tau_{turb} = \rho\nu \frac{\partial}{\partial z}\vec{u} \tag{74}$$

we obtain from (70) in the steady state the complex boundary value problem

$$\frac{d}{dz}\left(\rho\nu \frac{d}{dz} W\right) - i\rho f W = -i\rho f\left(u_{surf} - u_{stokes}\right)$$

$$w \to 0 \text{ for } |z| \to \infty. \tag{75}$$

Here, u_{surf} and u_{stokes} are given by (58) and (59), respectively. We confine our interest to the water column and ignore the motion in air, except that we impose a surface stress $\tau_a = \rho_a u_*^2 = \rho_w w_*^2$ caused by wind blowing in the x-direction. Here, u_* and w_* are the friction velocity in air and water respectively. The surface drift is singular, and hence we write

$$u_{surf} = \hat{u}_{surf}\delta(z), \ \hat{u}_{surf} = 2\omega|\hat{\eta}|^2. \tag{76}$$

Integration of the differential equation across the air-water interface therefore gives a contribution of the surface drift to the boundary condition. Hence,

$$\rho\nu\frac{d}{dz}W = \tau_a + 2if\rho\hat{u}_{surf} \text{ at } z = 0 \tag{77}$$

which implies that one can model the effects of the surface drift by simply modifying the boundary conditions at the surface.

Using the boundary condition (76) it is straightforward to find the appropriate solution to Eq. (75). Introducing the Ekman depth $\delta_E = \sqrt{2\nu/f}$ one finds

$$\begin{aligned} W &= \frac{2}{(1+i)\delta_E}\left(\frac{w_*^2}{f} + i\frac{\hat{u}_{surf}}{N}\right)e^{(1+i)z/\delta_E} \\ &\quad -\frac{2k\hat{u}_{surf}}{N}e^{2kz}, \end{aligned} \tag{78}$$

where $N = 1 + 2i(k\delta_E)^2$. From this solution it is seen that, apart from the Ekman depth δ_E the waves introduce another length scale, namely the Stokes depth $\delta_S = 1/2k$. More importantly though, the effect of the waves on the ocean current is felt throughout the whole Ekman depth. This is discussed in more detail by Polton et al (2003).

The Ekman transport becomes

$$T = \int_{-\infty}^{0} dz \ \rho_w W = -i\rho_w w_*^2/f \tag{79}$$

which, as expected, is independent of the wave drifts.

The classical Ekman solution is obtained by putting u_{surf} to zero in Eq. (78). At the surface this will give rise to a current which has an angle of $45\deg$ to the right of the stress direction. It is of interest to study the effect of the surface and Stokes drift on the Ekman spiral. This is shown in Fig. (10) where we have plotted the y-component of the velocity versus the x-component, normalized with the water friction velocity, for increasing depth. Note that, as expected from the boundary conditions, the deep ocean corresponds to vanishing current velocity. The particular case we have chosen is from Polton et al (2003): $w_* = 0.0061\text{m/s}$, $\nu = 0.0116\text{m}^2/\text{s}$, $f = 10^{-4}\text{s}^{-1}$, $k = 0.0105\text{m}^{-1}$ and $U_{stokes} = 0.068\text{m/s}$. With respect to the classical Ekman spiral the wave drifts give rise to less turning in the surface layer of the ocean while there is more turning in the deeper layers of the ocean. Nevertheless, with the choice of a constant eddy viscosity model, there is only a modest impact of the wave drifts on the Ekman spiral.

There is, however, a curious feature of the solution (78), which deserves further attention. The turbulent eddies

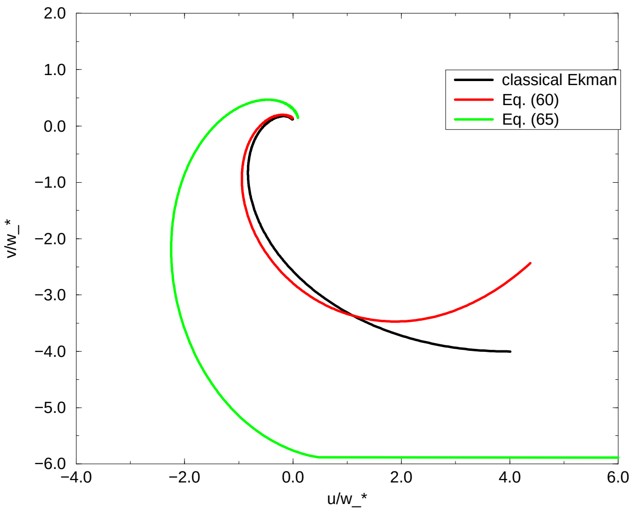

Figure 10: Ekman spiral for case of constant eddy viscosity. A comparison is made between two different treatments of the interaction of the surface drift and turbulence.

transport the momentum in the surface drift over the whole Ekman layer, as if the wave motion at the surface is almost completely destroyed by turbulent diffusion. This is odd since, as argued in section 3.1.1, the surface drift is a purely kinematical effect. This drift is simply present because of the combination of wave motion and the density jump at the surface. Therefore, as the other extreme, it may be more appropriate to apply turbulent diffusion only to the difference velocity $\vec{u} - \vec{u}_{surf}$.

Therefore, as an alternative to the turbulence model (74) we introduce the following parametrisation for turbulent stress:

$$\tau_{turb} = \rho\nu\frac{\partial}{\partial z}\vec{u}_c \tag{80}$$

where $\vec{u}_c = \vec{u} - \vec{u}_{surf}$, where $\vec{u}_c$ corresponds to the mean ocean circulation current $\vec{U}_c$ of section 3.1.1. The relevant boundary problem for $W_c = u_c + iv_c$ becomes

$$\begin{aligned} \frac{d}{dz}\left(\rho\nu\frac{d}{dz}W_c\right) - i\rho f W_c = i\rho f u_{stokes} \\ W_c \to 0 \text{ for } |z| \to \infty. \end{aligned} \tag{81}$$

Again confining our interest to the water column, we impose a surface stress $\tau_a = \rho_w w_*^2$, which results in the boundary condition

$$\rho\nu\frac{d}{dz}W_c = \tau_a \text{ at } z = 0. \tag{82}$$

The solution for the velocity $W = u + iv$ is then obtained by simply adding the surface drift to the solution for W_c. As a consequence we find

$$\begin{aligned} W &= u_{surf} \\ &\quad + \frac{2}{(1+i)\delta_E}\left(\frac{w_*^2}{f} + 2(k\delta_E)^2\frac{\hat{u}_{surf}}{N}\right)e^{(1+i)z/\delta_E} \end{aligned}$$

$$-\frac{2k\hat{u}_{surf}}{N}e^{2kz}, \tag{83}$$

where again $N = 1 + 2i(k\delta_E)^2$. Note that Polton et al (2003) obtained the same solution as above, except that they did not include the surface drift u_{surf}. Therefore, in the deeper layers of the ocean we obtain the same current profiles as Polton et al (2003). However, the latter authors find considerable deviations from the classical Ekman transport result, while, by inclusion of the surface contribution, we find that there are no deviations from the classical result. Integration of (83) over depth therefore gives (79).

With the present model for turbulence there are considerable deviations from the classical Ekman profile, as shown in Fig. (10) (note that in this figure we used the continuous version of the surface drift, Eq. (29). At the surface the Ekman turning is now about $10\,\deg$, hence much less than the classical $45\,\deg$-result, while in the deeper layers of the ocean there is considerably more turning. The important point to note here is that Polton et al (2003) have shown that the above solution shows impressive agreement with observed current profiles at depths of the order of the Ekman depth δ_E.

It is concluded from the present study that the inclusion of the surface and Stokes drift may have important implications for ocean circulation which certainly deserve further exploration. However, it is important to try to understand why the turbulence model (80) is the most appropriate, i.e. why the momentum in the surface drift is not diffused by turbulence to the deeper layers of the ocean. Nevertheless, the present study suggests that there are at least three length scale relevant in this problem, namely the Ekman depth δ_E, the Stokes depth δ_S and the significant wave height H_S as this is the relevant length scale for the surface drift.

3.2 *Impact of ocean currents on atmospheric fluxes.*

As was shown by Pacanowski (1987) inclusion of currents in the determination of the atmospheric fluxes results in considerable impact on the ocean circulation and the temperature distribution in the equatorial region. This can be readily seen as the wind speeds in that area are typically $6\ m/s$ while the surface currents can reach values of up to $1\ m/s$, hence differences in the momentum flux may be up to 30%.

Again, feedback from the ocean circulation to the atmosphere was not taken into account so that the results of Pacanowski (1987) may overstate the case. In order to investigate the size of the impact of the inclusion of currents in the flux determination, the boundary condition of zero velocity over the oceans in the IFS atmospheric code was replaced by one of a finite current as given by the ocean circulation model. We ran 6 months forecasts with this modified version of the ECMWF seasonal forecasting system over the period of 1991 until 2002. The forecasts started in January and July. There was a beneficial reduction of

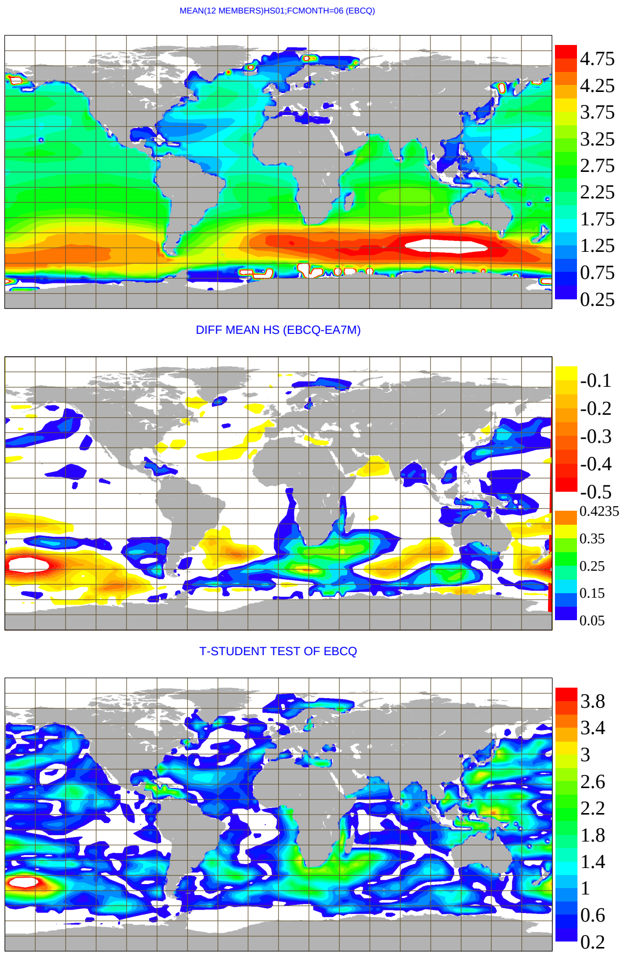

Figure 11: Impact of currents on fluxes as reflected by differences in the monthly mean wave height field. Top panel: mean of sixth month experimental forecast for July averaged over the 12 July's over the period 1991-2002. Middle panel: Difference with control. Bottom panel: significance parameter T; if $T > 2$ then the difference is significant with probability of 95%.

the drift in SST in the Equatorial Pacific, but the size of the reduction was only $0.1\,\deg K$. Nevertheless, there may be considerable differences in physical parameters such as the surface wind speed or significant wave height. This is shown in Fig. 11 which gives the monthly wave height field for the 6 month experimental forecast for July averaged over the twelve year period. In addition is shown the difference with the corresponding field of the control forecast, and the result of a significance test. There are considerable differences in the wave height field of the southern Hemisphere extra-tropics, and in the warm pool area east of Indonesia. The student t-test in the bottom panel reveals all of the major current systems of the ocean, except perhaps the Gulf stream in the North Atlantic.

In the work of Pacanowski (1987) and our experiments the ocean surface current was approximated by means of the current at $5\ m$ depth. However, it is known that this is a poor approximation; ocean waves play an important role in the top layer of the ocean, resulting in an additional surface drift of about 2.5% of the surface wind speed. In addition, because of Ekman turning, there may be considerable differences between the direction of the surface current and the one at $5\ m$ depth. These effects can, however, only be taken into account by using sea state information within the context of a coupled ocean-circulation, atmosphere model.

3.3 Surface layer mixing and ocean waves.

The work of Terray et al (1996) and Craig and Banner (1994) has highlighted the prominent role of breaking waves and its contribution to the surface current. For example, in the field considerable deviations from the usual balance between production and dissipation of turbulent kinetic energy are found which are caused by the energy flux produced by breaking waves. When observed turbulent kinetic energy dissipation, ϵ, and depth z are scaled by parameters related to the wave field, an almost universal relation between dimensionless dissipation and dimensionless depth is found. Here, dimensionless dissipation is given by $\epsilon H_S/\Phi_{aw}$, with H_S the significant wave height and Φ_{aw} the energy flux from wind to waves, while the dimensionless depth is given by z/H_S.

In the Craig and Banner model (1994) the difference between production and dissipation of turbulent kinetic energy is balanced by a flux of turbulent energy, following the work of Mellor and Yamada (1982). In particular, by choosing a wave-height dependent mixing length, Terray et al (1999) found a good agreement between modelled dissipation and current profile on the one hand and observations on the other hand.

In order to be able to give a realistic representation of the mixing processes in the surface layer of the ocean, it is clear that a reliable estimate of energy and momentum fluxes to the ocean column is required. A first attempt to estimate these fluxes from modelled wave spectra and knowledge about the generation and dissipation of ocean waves was given by Komen (1987). Weber (1994) studied energy and momentum fluxes in the context of a low-resolution coupled ocean-wave atmosphere model (WAM-ECHAM), and she concluded that there is no need to use a wave prediction model to determine, for example, the energy flux. A parametrization of the type $\Phi_{aw} = m\rho_a u_*^3$ (with u_* the air friction velocity and m a constant) would suffice. It will be argued that this conclusion depends on an approximation used by Weber to estimate the energy flux.

Let us first define the momentum and energy flux. The total wave momentum $\vec{P}$ depends on the variance spectrum $F(\omega,\theta)$ and is defined as

$$\vec{P} = \rho_w g \int_0^{2\pi} \int_0^{\infty} d\omega d\theta\ \frac{\vec{k}}{\omega} F(\omega,\theta), \tag{84}$$

which agrees with the well-known relation that wave momentum is simply wave energy divided by the phase speed of the waves. The momentum fluxes to and from the wave field are given by the rate of change in time of wave momentum, and one may distinguish different momentum fluxes depending on the different physical processes. For example, making use of the energy balance equation (1) the wave-induced stress is given by (cf. 2)

$$\vec{\tau}_{aw} = \rho_w g \int_0^{2\pi} \int_0^{\infty} d\omega d\theta\ \frac{\vec{k}}{\omega} S_{in}(\omega,\theta), \tag{85}$$

while the dissipation stress is given by

$$\vec{\tau}_{wo} = \rho_w g \int_0^{2\pi} \int_0^{\infty} d\omega d\theta\ \frac{\vec{k}}{\omega} S_{diss}(\omega,\theta), \tag{86}$$

Similarly, the energy flux from wind to waves is defined by

$$\Phi_{aw} = \rho_w g \int_0^{2\pi} \int_0^{\infty} d\omega d\theta\ S_{in}(\omega,\theta), \tag{87}$$

and the definition for Φ_{wo} follows immediately from the above one by replacing S_{in} by S_{diss}. It is important to note that while the momentum fluxes are mainly determined by the high-frequency part of the wave spectrum, the energy flux is to a larger extent determined by the low-frequency waves.

In an operational wave model, the prognostic frequency range is limited by practical considerations such as restrictions on computation time, but also by the consideration that the high-frequency part of the dissipation source function is not well-known. In the ECMWF version of the WAM model the prognostic range of the wave spectrum is given by the condition

$$\omega < \omega_c = 2.5\omega_{mean} \tag{88}$$

where ω_{mean} is a conveniently defined mean angular frequency. In the diagnostic range, $\omega > \omega_c$, the wave spectrum is given by Phillips' ω^{-5} power law. In the diagnostic range it is assumed that there is a balance between wind input, dissipation and nonlinear transfer. In practice this means that all energy and momentum going into the high-frequency range of the spectrum is dissipated, and is therefore directly transferred to the ocean column.

As a consequence, the momentum flux to the ocean, $\vec{\tau}_{oc}$, is given by

$$\begin{aligned} \vec{\tau}_{oc} &= \vec{\tau}_a \\ &-\rho_w g \int_0^{2\pi} \int_0^{\omega_c} d\omega d\theta\ \frac{\vec{k}}{\omega} \left(S_{in} + S_{nl} + S_{diss}\right), \end{aligned} \tag{89}$$

where $\vec{\tau}_a$ is the atmospheric stress, whose magnitude is given by $\tau_a = \rho_a u_*^2$. Note that the ocean momentum flux $\vec{\tau}_{oc}$ only involves the sum of the three source functions of the energy balance equation and therefore it only involves the total rate of change of wave momentum. Any wave model that is forced by reliable atmospheric stresses and that produces wave height results that compare well with, for example, buoy wave height data and Altimeter wave height data, will produce reliable estimates of the ocean momentum flux $\vec{\tau}_{oc}$.

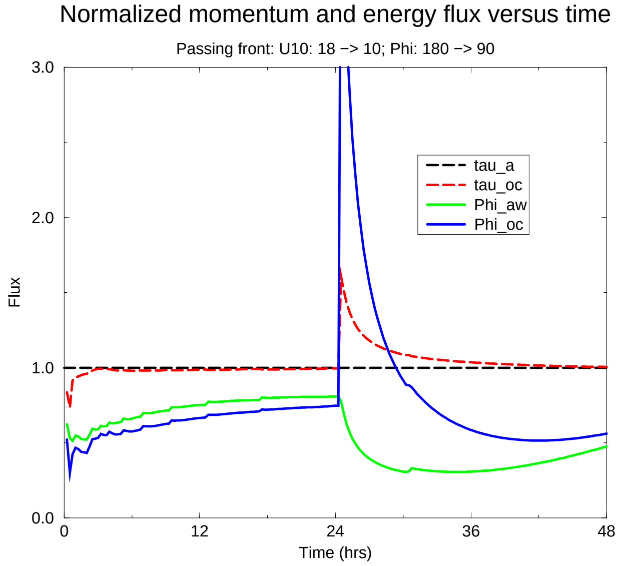

Figure 12: Evolution in time of normalized momentum flux and energy flux to the ocean for the case of a passing front after 24 hrs. The momentum flux has been normalized with $\rho_a u_*^2$, while the energy flux has been normalized with $m\rho_a u_*^3$, where $m = 5.2$.

Ignoring the direct energy flux from air to currents, because it is small (cf. Phillips, 1977), the energy flux to the ocean, Φ_{oc}, is given by

$$\Phi_{oc} = \Phi_{aw}^{tot} \\ -\rho_w g \int_0^{2\pi} \int_0^{\omega_c} d\omega d\theta \ (S_{in} + S_{nl} + S_{diss}), \quad (90)$$

where Φ_{aw}^{tot} is the total energy flux transferred from air to ocean waves. This total energy flux is fairly well-known, because empirically the wind input to ocean waves is well-known, even in the high-frequency part of the spectrum (cf. Plant, 1982). Furthermore, there is now a consensus that the high-frequency part of the spectrum obeys an ω^{-5} power law (Banner, 1990; Birch and Ewing, 1986; Hara and Karachintsev, 2003, to mention but a few references). Hence, fairly reliable estimates of the energy flux Φ_{oc} may be provided by means of a wave model provided the model has a wind input term that agrees with the observations of wave growth and provided modelled wave heights compare well with observations.

Before results of time series for momentum and energy flux for a simple case are presented, we have to make one remark on the numerical implementation of (89) and (90). The energy balance equation is solved by means of an implicit integration scheme (cf. Komen et al, 1994). To be consistent with the numerical treatment of the energy balance, the momentum and energy flux have to be treated in a similar spirit, i.e. including the implicit factors of the integration scheme.

Let us now illustrate the sea-state dependence of the momentum and energy flux for the simple case of the passage of a front. To that end we take a single grid-point version of the ECMWF version of the WAM model and force the waves for the first day with a constant wind speed of 18 m/s, which is followed by a drop in wind speed to 10 m/s and a change in wind direction by $90\,\deg$. In Fig. 12 we have plotted time series of atmospheric stress (τ_a), the momentum flux to the ocean (τ_{oc}), the total air-wave energy flux (Φ_{aw}^{tot}) and the energy flux into the ocean (Φ_{oc}). The momentum fluxes have been normalized by τ_a, while the energy fluxes have been normalized by $m\rho_a u_*^3$, with $m = 5.2$ which is a convenient mean value. During the first day we deal with the case of wind-generated gravity waves, hence windsea, and, in particular, the difference between atmospheric stress and the momentum flux to the ocean is small, most of the time at best 2%. This is a well-known property of windsea (JONSWAP, 1973). For windsea, the difference between total energy flux Φ_{aw}^{tot} and the energy flux into the ocean Φ_{oc} is somewhat larger. When the front passes at $T = 24\ hrs$ there is a sudden drop in wind, hence in atmospheric stress. However, the waves are still steep and experience an excessive amount of dissipation in such a way that wave energy decreases. As a consequence, considerable amounts of momentum and energy are dumped in the ocean column, much larger than the amounts one would expect from the local wind. Therefore, in cases of rapidly varying circumstances, the fluxes are seen to depend on the sea state. This is in particular true for the energy flux Φ_{oc} and to a much lesser extent for the momentum flux τ_{oc}.

This different behaviour of momentum flux and energy flux is caused by a combination of two factors. By definition momentum flux is mainly determined by the high frequency part of the spectrum while we have assumed that in the unresolved part of the spectrum there is a balance between wind input and dissipation. Hence, for windsea there is almost always a balance between atmospheric momentum flux and the flux into the ocean. This holds to a lesser extent for the energy flux because this flux is partly determined by the low frequency part of the wave spectrum as well.

The different behaviour of momentum and energy flux is also found in the monthly means on a global scale. This is illustrated in

the Figs. (13) and (14). The typical variation in the ratio τ_{oc}/τ_a is then found to be of the order of 4% while the variation in the normalized energy flux, $\Phi_{oc}/m\rho_a u_*^3$, is substantially larger. The global average of the value for m turns out to be $m \simeq 5.2$. Note that the map for the energy flux shows an interesting spatial pattern. In the equatorial region values of the normalized energy flux are small, suggesting that the mixed layer is thinner than the norm. In the extra-Tropics the normalized energy flux is considerably larger, presumably because here there is larger variability in the wind field.

We finally remark that in the work of Weber (1994) the energy flux into the ocean was approximated by the relation $\Phi_{oc} \simeq \langle c \rangle \tau_{aw}$, where $\langle c \rangle$ is the mean phase velocity. This generally overestimates the energy flux by at least a factor of two and as a consequence she finds fairly high values of m, $m \simeq 14$. In addition, in interesting cases such as

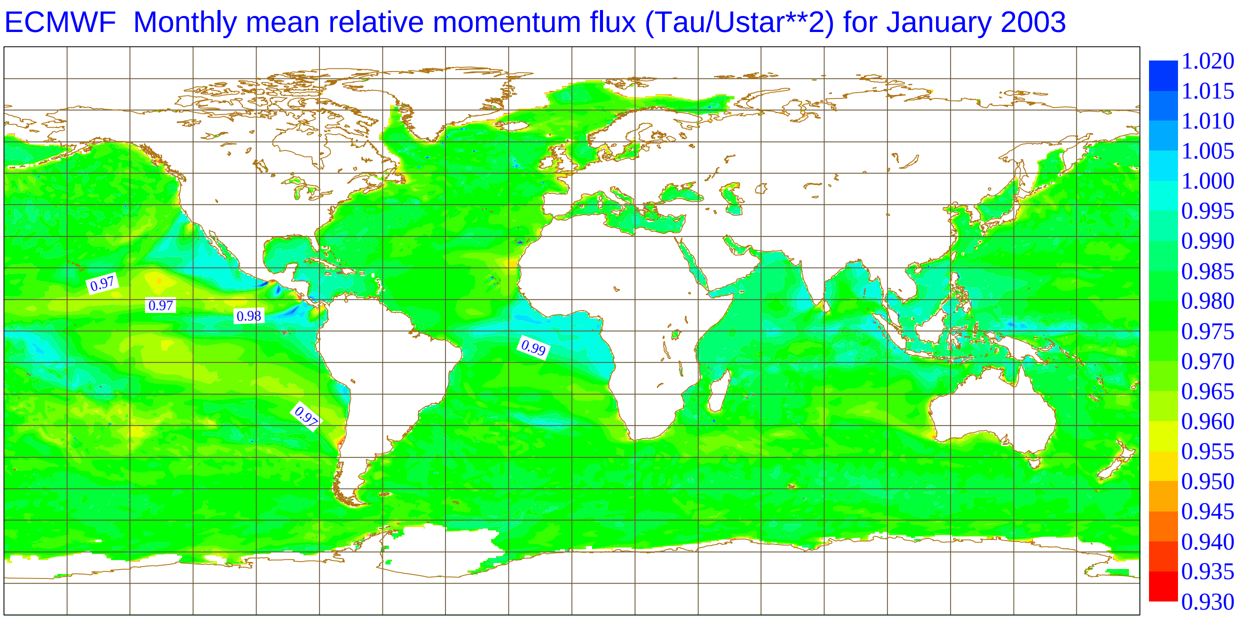

Figure 13: Monthly mean of momentum flux into the ocean, normalized with the atmospheric stress. Period is January 2003.

the passage of a front, the energy flux approximated in this manner will follow the wind. For example, in the frontal case of Fig. (12) the energy flux to the ocean would decrease dramatically at $T = 24$ hrs, while, in fact, it should hardly change. Therefore, it is not surprising that with this approximation the energy flux Φ_{oc} and wind are closely related.

3.4 *Mixed layer modelling.*

Having found a reliable way of obtaining from the rate of change of the wave spectrum the momentum and energy flux into the ocean, we now turn our attention to the consequences for the mean flow in the ocean. We follow the work of Craig and Banner (1994) and Mellor and Yamada (1982) and we briefly discuss the momentum equation, where the eddy viscosity is modelled in terms of the turbulent kinetic energy budget. In the steady state an exact solution is found for the case of no earth-rotation and no buoyance effects, but the mixing length may be arbitrary.

Momentum equation. To simplify the problem, the wind driven water velocity is assumed to be stationary, non-rotating and uniform without any pressure gradients in the horizontal directions. The momentum equation then reduces to

$$\frac{d}{dz}\left(\nu \frac{du}{dz}\right) = 0 \qquad \text{for} \qquad z \geq 0, \tag{91}$$

where for convenience we have taken increasing depth in the positive z-direction. The boundary conditions are:

$$\nu \frac{du}{dz} = -w_*^2 \qquad \text{for} \qquad z = 0, \tag{92}$$

$$u = 0 \qquad \text{for} \qquad z = H. \tag{93}$$

Here, u is the horizontal velocity component in x-direction. The eddy viscosity ν is assumed to be a function of depth only, w_* is the friction velocity in water and H is the total water depth. The friction velocity of water is related to the momentum flux according to

$$\tau_{oc} = \rho_w w_*^2 \tag{94}$$

Using (91) and (92), the stress in the water is found to be constant. The equation for the horizontal velocity then becomes

$$\frac{du}{dz} = -\frac{w_*^2}{\nu} \tag{95}$$

For given eddy viscosity, the velocity profile of the mean flow becomes

$$u = -w_*^2 \int_H^z \frac{dz}{\nu}. \tag{96}$$

The expression for ν will follow from the turbulent kinetic energy budget of the flow.

Kinetic energy equation. The equation for the mean kinetic energy of the turbulent velocity fluctuations is obtained from the Navier-Stokes equations. If buoyancy effects are ignored, and stationary two-dimensional flow is assumed, the energy budget becomes

$$0 = -w_*^2 \frac{du}{dz} + \frac{1}{\rho_w}\frac{d}{dz}(\overline{\delta p \delta w}) + \frac{d}{dz}(\overline{e \delta w}) - \varepsilon, \tag{97}$$

where ρ_w is the water density, δp and δw are the pressure and vertical velocity fluctuations, e is the turbulent kinetic energy and ε is the dissipation rate. The over-bar denotes the average taken over a time scale that removes linear turbulent fluctuations. Following Craig and Banner (1994), the level-$2\frac{1}{2}$ Mellor-Yamada turbulence scheme is

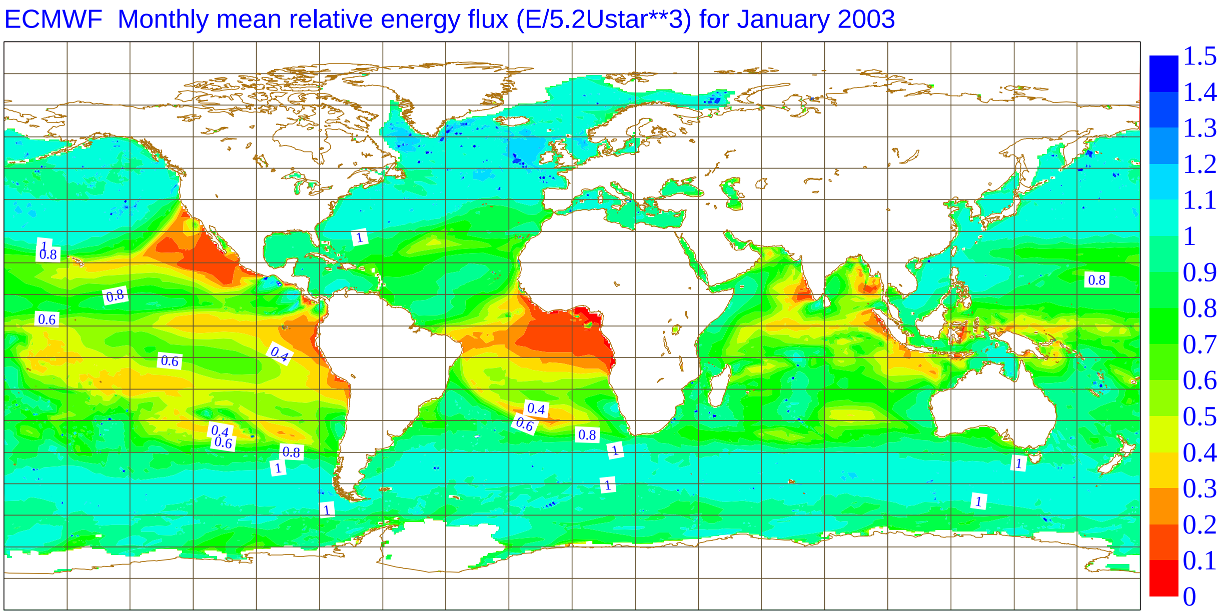

Figure 14: Monthly mean of energy flux into the ocean, normalized with $m\rho_a u_*^3$ where $m \simeq 5.2$. Period is January 2003.

used (Mellor and Yamada 1982). Here, the eddy viscosity is expressed as

$$\nu = lqS_M \tag{98}$$

where l is the turbulent mixing length, q^2 is the turbulent kinetic energy (q is referred to as the turbulent velocity) and S_M is a dimensionless constant. The dissipation term is taken to be proportional to the cube of the turbulent velocity divided by the mixing length

$$\varepsilon = \frac{q^3}{Bl}, \tag{99}$$

Here, B is another dimensionless constant. In the Mellor-Yamada scheme, the terms for the vertical transport of turbulent kinetic energy are parametrized through a diffusion term. Using the equation for the velocity profile (95) to eliminate the velocity shear, the equation for q becomes

$$-\frac{d}{dz}\left(\frac{1}{3}lS_q\frac{dq^3}{dz}\right) = \frac{w_*^4}{lqS_M} - \frac{q^3}{Bl} \tag{100}$$

where S_q is a constant. The term on the left-hand side of (100) represents vertical diffusion of turbulent kinetic energy. The first term on the right side is the shear production of turbulent kinetic energy, and the final term on the right side represents dissipation of turbulent energy. The boundary conditions for the turbulent kinetic energy equation are

$$-\frac{1}{2}lqS_q\frac{dq^2}{dz} = F_0 \quad \text{for} \quad z = 0, \tag{101}$$

$$\frac{dq^2}{dz} = 0 \quad \text{for} \quad z = H. \tag{102}$$

The values used in the empirical constants of the Mellor-Yamada model are

$$(S_M, S_q, B) = (0.39, 0.2, 16.6) \tag{103}$$

In order to agree with the turbulence results in case there is a balance between production and dissipation of kinetic energy the parameters S_M and B satisfy the relation $B^{1/4}S_M^{3/4} = 1$.

The energy flux $\rho_w F_0$ is related to the energy flux into the ocean by

$$\rho_w F_0 = \Phi oc \tag{104}$$

In the absence of the relevant information on the sea state, the energy flux is often parametrized as $\Phi oc = m\rho_a u_*^3$. Hence writing,

$$F_0 = \alpha w_*^3, \tag{105}$$

one then finds $\alpha = m\,(\rho_w/\rho_a)^{1/2}$. With m of the order of $2-5$, α has typical values of $50-150$.

Note, that we still need to specify the mixing length, l. Before this is done, we will study in the next section the diffusion problem for arbitrary mixing lengths.

Exact solution of the diffusion problem. In this section we present the exact solution to the diffusion problem (100)-(102). Let

$$q = w_*\left(\frac{B}{S_M}\right)^{1/4} y \qquad \text{and} \qquad w = y^3. \tag{106}$$

Furthermore, introduce a new length scale x,

$$dx = \frac{dz}{l\sqrt{\frac{1}{3}S_qB}} \qquad \Rightarrow \qquad x = \int \frac{dz}{l\sqrt{\frac{1}{3}S_qB}} \tag{107}$$

in such a way that $z = 0$ corresponds to $x = 0$, and $z \to \infty$ when $x \to \infty$. As a consequence, (100)-(102) becomes

$$\begin{aligned} x \geq 0: \ \frac{d^2w}{dx^2} &= w - w^{-1/3} \\ x = 0: \ \frac{dw}{dx} &= -\Phi_0 \\ w \to 1 &\text{ for } x \to \infty \end{aligned} \tag{108}$$

where $\Phi_0 = \sqrt{3} S_M^{3/4} \alpha / B^{1/4} S_q^{1/2}$.

The set of equations (108) can be solved exactly because there is an integral of motion. Multiplying the non-linear differential equation for w by dw/dx and integrating, we get

$$\left(\frac{dw}{dx}\right)^2 = w^2 - 3w^{2/3} + \mathrm{const} \qquad (109)$$

The integration constant is determined from the boundary condition at $z \to \infty$ ($w \to 1$ hence $dw/dx \to 0$) giving $\mathrm{const} = 2$, hence

$$\left(\frac{dw}{dx}\right)^2 = w^2 - 3w^{2/3} + 2 \qquad (110)$$

In principle an explicit solution is now obtained. To see this we write (110) as an equation for dx/dw and take the square root, hence

$$\frac{dx}{dw} = \pm \frac{1}{\sqrt{w^2 - 3w^{2/3} + 2}} \qquad (111)$$

and for definiteness we need the value of w at the surface. Using (110) and the boundary condition in (108) we get

$$w_0^2 - 3w_0^{2/3} + 2 - \Phi_0^2 = 0 \qquad (112)$$

Integration of (111) then gives

$$x = \int_{w_0}^{w} \frac{dw}{\sqrt{w^2 - 3w^{2/3} + 2}} \qquad (113)$$

Denoting the primitive integral by $J(w)$, so that

$$J = \int \frac{dw}{\sqrt{w^2 - 3w^{2/3} + 2}} \qquad (114)$$

(an explicit form will be given later), we therefore find

$$x = J(w) - J(w_0) \qquad (115)$$

where w_0 follows from (112).

Next, we solve the equation for $u(z)$. In terms of the x-coordinate, equation (92) becomes, using $u(z) = w_* u_0(z)$,

$$x \geq 0: \; w^{1/3} \frac{du_0}{dx} = -\tau_0^{1/2}, \qquad (116)$$

where $\tau_0^{1/2} = S_q^{1/2} B^{1/4} / \sqrt{3} S_M^{3/4}$, while the boundary condition becomes

$$x = H: \; u_0 = 0, \qquad (117)$$

Hence

$$u_0 = -\tau_0^{1/2} \int \frac{dx}{w^{1/3}} \qquad (118)$$

Using (111) we may write the integral in terms of w only, or

$$u_0 = -\tau_0^{1/2} \int \frac{dw}{w^{1/3}\sqrt{w^2 - 3w^{2/3} + 2}} \qquad (119)$$

This integral can be solved immediately by means of the substitution $w^{2/3} = y + 1$, with the final result

$$u_0 = \frac{3}{2\sqrt{3}} \tau_0^{1/2} \log \left(\frac{\sqrt{w^{2/3}+2} - \sqrt{3}}{\sqrt{w^{2/3}+2} + \sqrt{3}} \right) \Bigg|_{w_H}^{w} \qquad (120)$$

Therefore, the current u_0 has been expressed in terms of w.

The remaining task is now to determine w_H. For this we need the integral (114). Using $w = v^3$ one finds

$$\begin{aligned} J &= 3 \int \frac{v^2 dv}{(v^2-1)\sqrt{v^2+2}} \\ &= 3 \left(\int \frac{dv}{\sqrt{v^2+2}} + \int \frac{dv}{(v^2-1)\sqrt{v^2+2}} \right) \end{aligned} \qquad (121)$$

Both integrals are known and the end result is

$$\begin{aligned} J &= \frac{\sqrt{3}}{2} \log \left(\frac{1}{2} \left\{ \frac{\sqrt{3} w^{1/3} - \sqrt{w^{2/3}+2}}{\sqrt{3} w^{1/3} + \sqrt{w^{2/3}+2}} \right\} \right) \\ &+ 3 \log \left(w^{1/3} + \sqrt{w^{2/3}+2} \right) \end{aligned} \qquad (122)$$

In the exact solution for the diffusion problem a key role is played by the variable w. First one has to obtain the surface value of w from the solution of Eq. (112) Then, for given w the coordinate x can be obtained using (115) and (122). The values for z are then found by inverting (107), or,

$$z = \sqrt{\frac{1}{3} S_q B} \int l dx, \qquad (123)$$

and the current profile is found immediately from (120).

What remains now is the study of the roots of (112). It is convenient to introduce the variable $y = w^{2/3}$, which is basically the turbulent kinetic energy. In terms of y one finds the third order equation

$$y^3 - 3y + 2 - \Phi_0 = 0 \qquad (124)$$

For $\Phi_0 > 4$ this equation has only one real positive root, while in the opposite case ($\Phi_0 \leq 4$) there are three real roots. One of the additional roots is always negative and, therefore, physically not meaningful, because the turbulent kinetic energy is positive. The other root becomes positive for $\Phi_0 < 2$. Accordingly, for weak forcing, when $\Phi_0 \leq 2$, two different equilibrium solutions are possible. The first solution results in values of $w_0 > 1$. For this solution w is decreasing asymptotically towards the deep water value 1. The other solution results in surface values $0 \leq w_0 \leq 1$. Since also this solution must comply with the deep water boundary condition, this results in increased turbulence with depth.

We have studied to some detail the properties of the multiple equilibria. Current profiles are very similar, but there are considerable differences in the dissipation of turbulent kinetic energy. However, since multiple solutions only exist for extremely weak forcing ($\Phi_0 \leq 2$), corresponding to

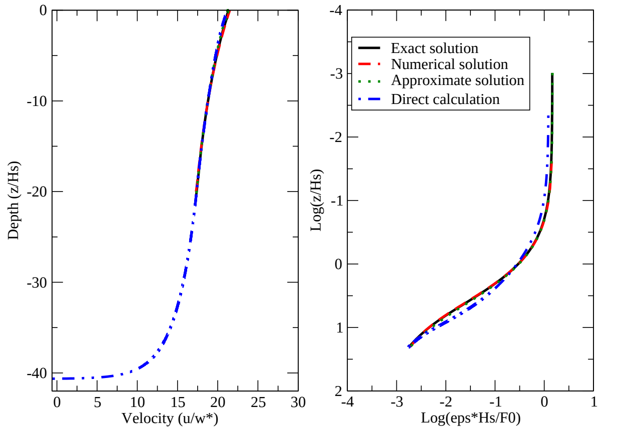

Figure 15: Velocity profile (left) and dissipation of turbulent kinetic energy (right) for exact, numerical, and approximate solution. The direct calculation uses the new model for turbulent kinetic energy, making use of the dissipation term of WAMcy4.

values of α of $\mathcal{O}(1)$, we have not pursued the consequences in great detail.

Fig. (15) shows current profile and dissipation rate (made dimensionless in an appropriate fashion) as function of dimensionless depth z/H_S for the case of $\alpha = 69$ and $H_S = 1.9\ m$. The mixing length scale l was chosen as

$$l(z) = \kappa(z + z_0), \quad z_0 = 1.6H_S.$$

The comparison between exact and numerically obtained solution is excellent.

The fact that the exact solution of equation (100) has to be calculated inversely, by first choosing w and finding the z values at the final stage, makes it a bit awkward for practical purposes. It is possible to find an approximate solution that is easier and faster to use which, for example, may be implemented in a numerical ocean model. The main difficulty in solving equation (100) is due to the non-linearity in the shear production term. Near the surface, the main balance is between the diffusion and the dissipation term, whereas for the deep layer, the balance is between the shear production and the dissipation term. Craig and Banner (1994) give the solutions for these two layers when the wave enhanced layer is assumed to be balanced by dissipation, and for the deep layer when the dissipation is balanced by shear production. The latter gives rise to the classical logarithmic velocity profile. It is, however, difficult to find an asymptotic matching between these two solutions. A rudimentary way of removing the non-linearity from equation (100), is by replacing q in the denominator of the shear production term by its deep water value. It is straightforward to solve the resulting linear problem and in Fig. (15) the resulting solution is compared with the exact one. A good agreement for current profile and dissipation rate is obtained.

Direct calculation of vertical transport. In the non-linear model for the ocean current in the surface layer, Eq.(100), the combined effects of the pressure term and the vertical transport of turbulent kinetic energy are modelled by means of a diffusion term. However, the pressure term can also be determined by explicitely modelling the energy transport caused by wave breaking. Janssen (1999) demonstrated how the pressure term may affect flow in the atmospheric boundary layer by explicitely using knowledge on the growth of waves by wind. The same idea will be used here but now applied to wave breaking in the ocean column. The pressure term is thus written as

$$I_w = +\frac{1}{\rho_w}\frac{d}{dz}(\overline{\delta p \delta w}) = -2g\int kS_{diss}(\vec{k})e^{-2kz}d\vec{k} \tag{125}$$

Neglecting the third order term involving the turbulent kinetic energy and using the same parametrizations for the dissipation and eddy viscosity as in the Mellor-Yamada model, the turbulent energy budget may be written as

$$q^4 - lBI_wq - \frac{Bu_*^4}{s_M} = 0 \tag{126}$$

Here, (95) has been used to eliminate the velocity gradient of the mean flow. With (126) and (100) we have two turbulence models that both involve the balance between vertical transport, shear production and dissipation of turbulent kinetic energy. The main difference is that the Mellor-Yamada model parametrizes the vertical flux of kinetic energy by a diffusion term while the new model calculates this term directly from the dissipation source function of the energy balance equation (1).

Let us explore the consequences of the turbulent kinetic energy equation (126) for current profile and dissipation rate profile. To that end, a one grid point version of the WAM model was run over a 24 hour period and the results at the end of the run were used for calculating the turbulence in the surface layer of the ocean and the resulting velocity profile. Wind speed was kept constant at 10 m/s during the whole run. At final time the significant wave height was 1.9 m and the waterside friction velocity w_* was 0.012 m/s. The energy flux for the boundary condition was calculated using (90), while I_w from (125) was obtained from the dissipation source function of the WAM model. Comparison with the results of the Mellor-Yamada model, run for the same conditions, are shown in Fig. (15). There is a remarkable agreement, taking into consideration the well-known uncertainties regarding the modelling of wave dissipation.

4 CONCLUSIONS.

In this paper we have reviewed the impact of the sea state on the atmospheric circulation, from the medium-range to seasonal forecasting time scales. An important finding is that with the recent increase of atmospheric resolution from T_l319 to T_l511 we have experienced a more pronounced impact of ocean waves on the atmosphere in the medium-range. The same remark applies to seasonal forecasting time scales. Apparently, a realistic representation of the small scales is important for air-sea interaction.

Furthermore, we have discussed possible benefits of sea state information for coupled atmosphere, ocean circulation modelling such as relevant for seasonal forecasting. These possible benefits have always been ignored by the ocean modelling community. This is surprising when it is realized from the physical point of view that the ocean surface layer is to a large extent controlled by the physics of breaking waves. This will have impact on the magnitude and direction of the surface drift, and hence on the atmospheric circulation and fluxes. In addition, the energy flux into the ocean is sea state dependent, and therefore also the thickness of the mixed layer. In particular, the mixed layer will be shallow in areas where there is hardly any variability in the wind, such as in the Trade winds, whereas the mixed layer will be deep in the extra-Tropics.

The study of the impact of ocean waves on ocean circulation is only beginning. There are nevertheless already some interesting results, e.g. the work of Mastenbroek et al (1993) on the impact of the sea-state dependent drag on the mean sea level and the work of Polton et al (2003) on the impact of the Stokes drift on the Ekman spiral. The next task is to obtain the relevant primitive equations, including the effect of surface waves. In the context of multi-layer models the approach of section 3.1.1 seems promising, where, because of its simplicity, there is a preference for evolution equations for the total horizontal velocity. The significant impact of the Stokes drift on the Ekman spiral is found when the turbulent stresses are parametrized by means of the mean ocean circulation velocity. This makes sense because the surface drift is highly concentrated near the air-sea interface. Near the ocean surface the momentum transport is to a large extent determined by the energy flux associated with breaking waves. A turbulence model to deal with such circumstances is a scheme developed by Mellor and Yamada (1982). In case of neutral stratification and no Coriolis force we have found an exact solution for the turbulent kinetic energy profile and the current profile. No doubt, this exact solution will be of help in parametrizing the mixing length near the surface.

Acknowledgment

The authors appreciate discussions with Dave Anderson, Martin Miller, Glenn Shutts and Anthony Hollingsworth. We thank Magdalena Balmaseda, Anton Beljaars and Tim Stockdale for their support and analysis of the current-fluxes experiment.

5 REFERENCES

[1] Andrews, D.G. and M.E. McIntyre, 1976. Planetary waves in horizontal and vertical shear: the generalized Eliassen-Palm relation and the mean zonal acceleration. *J. Atmos. Sci.* **33**, 2031-2048.

[2] Banner, M.L., 1990b. Equilibrium spectra of wind waves. *J. Phys. Oceanogr.* **20**, 966-984.

[3] Bidlot, Jean-Raymond, Holmes, Damian J., Wittmann, Paul A., Lalbeharry, Roop, Chen, Hsuan S. 2002. Intercomparison of the Performance of Operational Ocean Wave Forecasting Systems with Buoy Data. *Weather and Forecasting***17**, 287-310.

[4] Birch, K.G. and J.A. Ewing, 1986. Observations of wind waves on a reservoir, IOS-rep. No. 234, Wormley, 37p.

[5] Burgers, G.J.H., P.A.E.M. Janssen, and D.L.T. Anderson, 1995. Impact of sea-state dependent fluxes on the tropical ocean circulation. International Scientifi c Conference on the Tropical Ocean's Global Atmosphere (TOGAS), 2-7 April 1995, Melbourne, 295-297.

[6] Craig, P.D. and M.L. Banner,1994. Modeling wave-enhanced turbulence in the ocean surface layer. *J. Phys. Oceanogr.* **24**, 2546-2559.

[7] Doyle, J.D., 1995: Coupled ocean wave/atmosphere mesoscale simulations of cyclogenesis, *Tellus* **47A**, 766-778.

[8] Hara T, and A.V. Karachintsev, 2003. Observation of Nonlinear Effects in Ocean Surface Wave frequency Spectra. *J. Phys. Oceanogr.* **33**, 422-430.

[9] Hasselmann, K., 1970. Wave-driven inertial oscillations. *Geophys. Fluid Dyn.* **1**, 463-502.

[10] Hasselmann, K., 1971. On the mass and momentum transfer between short gravity waves and larger-scale motions. Part 1. *J. Fluid Mech.* **50**, 189-205.

[11] Hasselmann, K., T.P. Barnett, E. Bouws, H. Carlson, D.E. Cartwright, K. Enke, J.A. Ewing, H. Gienapp, D.E. Hasselmann, P. Kruseman, A. Meerburg, P. Müller, D.J. Olbers, K. Richter, W. Sell and H. Walden, 1973. Measurements of wind-wave growth and swell decay during the Joint North Sea Wave Project (JONSWAP), *Dtsch. Hydrogr. Z. Suppl. A* **8(12)**, 95p.

[12] Janssen, P.A.E.M., 1982. Quasilinear approximation for the spectrum of wind-generated water waves. *J. Fluid Mech.* **117**, 493-506.

[13] Janssen, P.A.E.M., 1989. Wave-induced stress and the drag of air fbw over sea waves. *J. Phys. Oceanogr.* **19**, 745-754.

[14] Janssen, P.A.E.M., 1991. Quasi-linear theory of wind wave generation applied to wave forecasting. *J. Phys. Oceanogr.* **21**, 1631-1642.

[15] Janssen, P.A.E.M., 1999. On the effect of ocean waves on the kinetic energy balance and consequences for the inertial dissipation technique. *J. Phys. Oceanogr.* **29**, 530-534.

[16] Janssen, P.A.E.M., and P. Viterbo, 1996. Ocean Waves and the atmospheric Climate. *J. Climate* **9**, 1269-1287.

[17] Janssen, P.A.E.M., J-R. Bidlot and B. Hansen, 2000. Diagnosis of the ECMWF ocean-wave forecasting system. ECMWF Technical Memorandum, **318**, Reading, U.K.

[18] Janssen, P.A.E.M., J.D. Doyle, J. Bidlot, B. Hansen, L. Isaksen and P. Viterbo, 2002: Impact and feedback of ocean waves on the atmosphere. in *Advances in Fluid Mechanics*, **33**, Atmosphere-Ocean Interactions ,Vol. I, Ed. W.Perrie.

[19] Jenkins, A.D., 1987a. A lagrangian model for wind- and wave-induced near-surface currents. *Coastal Engineering* **11**, 513-526.

[20] Jenkins, A.D., 1987b. Wind- and wave-induced currents in a rotating sea with depth-varying eddy viscosity. *J. Phys. Oceanogr.* **17**, 938-951.

[21] Komen, G.J., 1987. Energy and momentum fluxes through the sea surface. *Dynamics of the Ocean Surface Mixed Layer*, P. Müller and D. Henderson, Eds., Hawaii Institute of Geophysics Special Publications, 207-217.

[22] Komen, G.J., L. Cavaleri, M. Donelan, K. Hasselmann, S. Hasselmann, and P.A.E.M. Janssen, 1994: *Dynamics and Modelling of Ocean waves* (Cambridge University Press, Cambridge)

[23] Longuet-Higgins, M.S. and R.W. Stewart, 1961. The changes in amplitude of short gravity waves on steady non-uniform currents. *J. Fluid Mech.* **10**, 529-549.

[24] Mastenbroek, C., G.J.H. Burgers and P.A.E.M. Janssen, 1993. The dynamical coupling of a wave model and a storm surge model through the atmospheric boundary layer. *J. Phys. Oceanogr.* **23**, 1856-1866.

[25] McWilliams, J.C., and J.M. Restrepo, 1999. The wave-driven ocean circulation. *J. Phys. Oceanogr.* **29**, 2523-2540.

[26] Mellor, G.L. and T. Yamada, 1982. Development of a turbulence closure model for geophysical fluid problems. *Rev. Geophys. Space Phys.* **20**, 851-875.

[27] Pacanowski, R.C., 1987. Effect of Equatorial Currents on Surface Stress. *J. Phys. Oceanogr.* **17**, 33-838.

[28] Polton, J.E., D.M. Lewis, and S.E. Belcher, 2003. The role of wave-induced Coriolis-Stokes forcing on the wind-driven mixed layer. submitted to *J. Phys. Oceanogr.*.

[29] Phillips, O.M., 1977. The dynamics of the upper ocean, Cambridge University Press, Cambridge, 336p.

[30] Plant, W.J., 1982. A relation between wind stress and wave slope. *J. Geophys. Res.* **C87**, 1961-1967.

[31] Terray, E.A., M.A. Donelan, Y.C. Agrawal, W.M. Drennan, K.K. Kahma, A.J. Williams, P.A. Hwang, S.A., and Kitaigorodskii, 1996. Estimates of Kinetic Energy Dissipation under Breaking Waves. *J. Phys. Oceanogr.* **26**, 792-807.

[32] Terray, E.A., W.M. Drennan, and M.A. Donelan, 1999. The vertical structure of shear and dissipation in the ocean surface layer. *The wind-driven air-sea interface*, M.L. Banner, Ed., School of Mathematics, The University of New South Wales, Sydney, 239-245.

[33] Weber, J.E., 1983. Steady Wind- and Wave-induced currents in the open ocean. *J. Phys. Oceanogr.* **13**, 524-530.

[34] Weber, S.L., 1994. Statistics of the air-sea fluxes of Momentum and Mechanical energy in a Coupled wave-atmosphere model. *J. Phys. Oceanogr.* **24**, 1388-1398.

[35] Whitham, G.B. (1962). Mass, momentum and energy flux in water waves. *J. Fluid Mech.* **12**, 135-147.

[36] Whitham, G.B., 1974. *Linear and nonlinear waves*. Wiley, New York, 636p.

[37] Xu, Z., and A.J. Bowen, 1994. Wave- and wind-driven flow in water of finite depth. *J. Phys. Oceanogr.* **24**, 1850-1866.